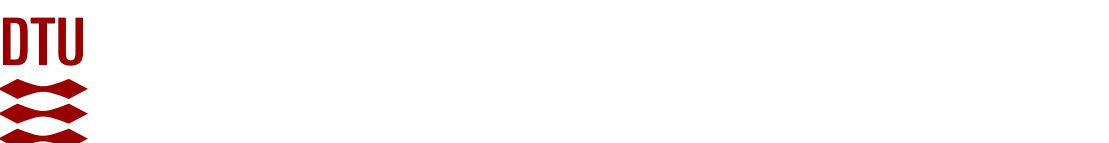
Downloaded from orbit.dtu.dk on: ,



DTU Library

Reuse of brine from desalination

Englmair, Gerald; Larsen, Anne Sofie ; Kong, Weiqiang; Vajda, Barney ; Meola, Alberto ; Furbo, Simon; Rygaard, Martin

Publication date: 2020

Document Version
Publisher's PDF, also known as Version of record

Link back to DTU Orbit

Citation (APA):

Englmair, G., Larsen, A. S., Kong, W., Vajda, B., Meola, A., Furbo, S., & Rygaard, M. (2020). Reuse of brine from desalination.

General rights

Copyright and moral rights for the publications made accessible in the public portal are retained by the authors and/or other copyright owners and it is a condition of accessing publications that users recognise and abide by the legal requirements associated with these rights.

- Users may download and print one copy of any publication from the public portal for the purpose of private study or research.
- You may not further distribute the material or use it for any profit-making activity or commercial gain
- You may freely distribute the URL identifying the publication in the public portal

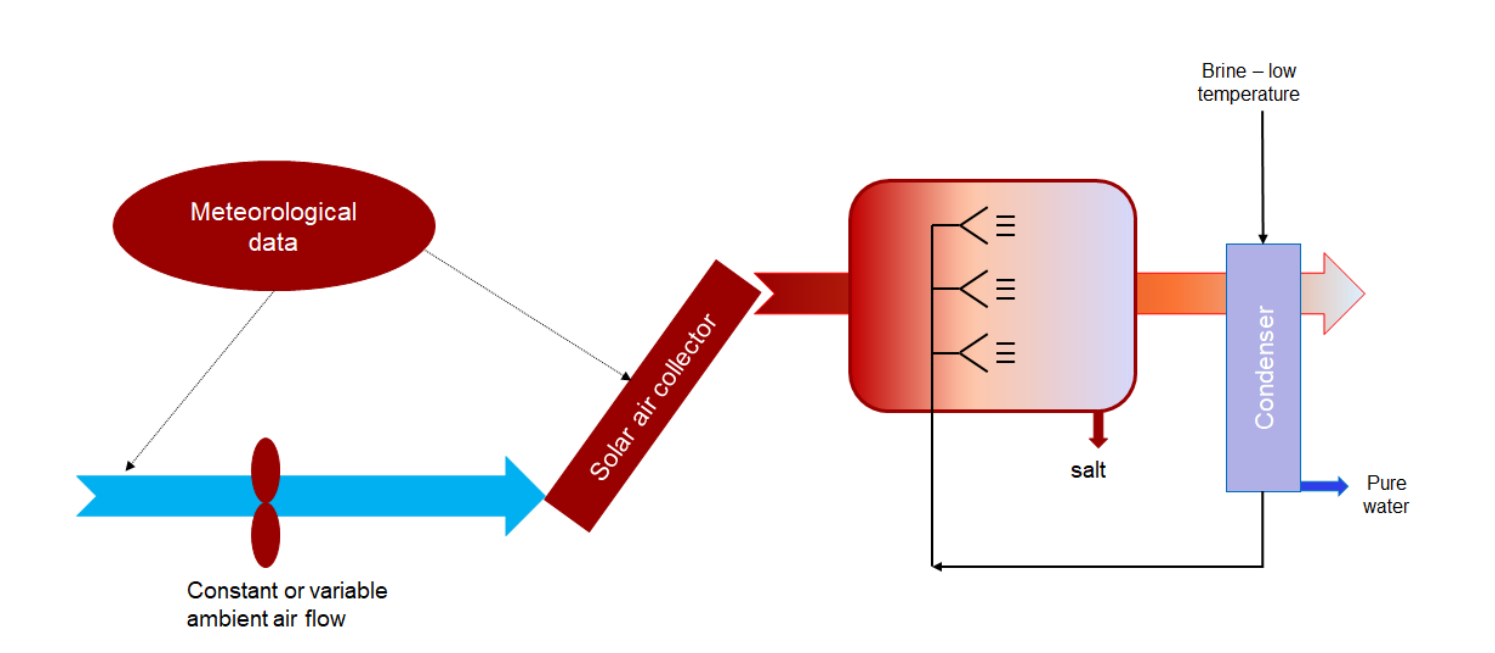
If you believe that this document breaches copyright please contact us providing details, and we will remove access to the work immediately and investigate your claim.



BYG R-446 October 2020

Reuse of brine from desalination (NoBriner)

Gerald Englmair, Anne Sofie Larsen, Weiqiang Kong, Barney Vajda, Alberto Meola, Simon Furbo, Martin Rygaard



Reuse of brine from desalination (NoBriner)

Report Byg R-446 October 2020

Ву

Gerald Englmair DTU Civil Engineering (corresponding author; gereng@byg.dtu.dk)
Anne Sofie Larsen, NoBriner (project lead; www.nobriner.org)
Weiqiang Kong, DTU Civil Engineering
Barney Vajda, NoBriner
Alberto Meola, NoBriner
Simon Furbo, DTU Civil Engineering
Martin Rygaard, DTU Environment

Copyright: Reproduction of this publication in whole or in part must include the customary

bibliographic citation, including author attribution, report title, etc.

Cover: Layout for simplified system investigations (source: DTU Civil Engineering)

Udgivet af: DTU Civil Engineering, Brovej, Bygning 118, 2800 Kgs. Lyngby

www.byg.dtu.dk

ISBN: 87-7877-5477



Preface

From February (project kick-off) until August 2020, researchers from DTU Byg and DTU Miljø assisted NoBriner by conducting literature investigations, by creating theoretical models to elucidate limitations of the aimed desalination system and by planning an experimental setup. NoBriner coordinated the work and contributed to the project with a strong focus on sustainable implementation and market exploration. Project communication was realized by monthly penal meetings to decide next work steps and additional working meetings. The project faced restrictions due to the COVID-19 pandemic. Thus, most meetings were held online and the work plan needed to be adopted in accordance with access rules at DTU.

The authors contributed to this report in the following way: Researchers from DTU Civil Engineering were responsible for the literature study, development of simulation models for NoBriner's spray evaporation unit, planning of experimental investigations as well as for numerical investigations on system integration of a spray evaporation unit. Martin Rygaard (DTU Environment) was responsible for inputs to brine characteristics. NoBriner was responsible for the sections on sustainable implementation, market exploration as well as for development of an assessment tool for solar electricity production. The assembly of the project report was coordinated by Gerald Englmair. All authors were involved in reviewing this report.

The authors would like to thank the Vand Innovation SMVer (VIS) program at DTU for enabling this work – financially supported from the European Union, European fond for regional development.

Copenhagen, August 2020

Anne Sofie Larsen (project lead)



Content

| Executive summary | 3 |
|--|----------------------------|
| Literature study on different desalination methods inclusive brine characteristics Definitions Technology overview in relation to spray evaporation Brine characteristics | 4 4 5 8 |
| Sustainable implementation Social aspects on implementation Investigations in Kenya Workshop Methodology for sustainable implementation of technology | 11 11 11 12 12 |
| Market exploration Market overview Potential applications cases | 13 14 15 |
| Development of simulation models for NoBriner´s spray evaporation unit Pure water spray evaporation model (Python) Brine spray evaporation model (Python) Parametric study of droplet evaporation TRNSYS water droplet evaporation model (type 1020) | 18 18 24 28 29 |
| Preparation of experimental investigations Test setup Component sizing Selected equipment and fist preparations at DTU Byg | 32 32 33 36 |
| System aspects Assessment tool: solar electricity production Numerical investigation on system integration of a spray evaporation unit | 39 39 44 |
| Conclusions | 48 |
| References | 50 |



Executive summary

NoBriner (www.nobriner.org) aims to develop a technology to manage brine, a byproduct from the desalination process when producing safe drinking water from saline water sources. As a solution, a zero-liquid discharge desalination method, based on spray evaporation, is targeted - as a stand-alone solution, which can be combined with various desalination processes and heat sources. Furthermore, for application in rural areas with poor access to infrastructure, the technology is required to be low maintenance.

Literature study was performed on characteristics of different desalination processes, with a focus on reference solutions for zero liquid discharge of brine as well as on system aspects in relation to the aimed NoBriner spray evaporation solution. Brine characteristics were determined experimentally (sample from Kenya) and by database screening.

Investigations on sustainable implementation focused on social aspects and available infrastructure, dependent on the location. Furthermore, reference solutions for brine utilization were studied. The potential market was explored for brine as a multifunctional product. NoBriner worked on business development regarding the outlook of potential clients and projects.

Zero-liquid discharge of brine was theoretically investigated by means of detailed models for droplet evaporation of pure water and brine. Literature findings were utilized to build and a standalone simulation program in Python. It was possible to verify the droplet evaporation model for pure water, which was utilized for experimental spray evaporation setup dimensioning. Thus, when brine is experimentally tested, the model can be updated in the future. To facilitate a future experimental validation of the zero-liquid discharge concept, DTU Byg planned an experimental spray evaporation setup. Components were selected and sized - at this stage the setup could be realized at DTU Byg after the necessary material (pipes, fittings, spraying equipment) is purchased.

Furthermore, NoBriner and DTU Byg developed models for extended theoretical investigations: a) Solar electricity production assessment – a python tool was developed; The solar electricity assessment tool was verified with a public database. It can be utilized for holistic planning of stand alone solutions requiring electricity to power fans and pumps.

b) system simulation utilizing solar thermal collectors – a TRNSYS spray evaporation model was developed. The TRNSYS model was successfully applied in a fist, simplified system scenario with a solar collector model and meteorological data from Nairobi, Kenya. Assumed parameters (performance of spray evaporation unit in dependency of ambient conditions) must be experimentally verified, then the model could be applied to design a spray evaporation system. Based on calculations results of the simplified system scenario, a stand-alone solution for zero liquid discharge is difficult to realise - experimental work is crucial to clarify applicability.

All project results are documented in this report. Collected literature, developed simulation models and calculation sheets were made available to NoBiner for further development of brine management solutions.



1. Literature study on different desalination methods inclusive brine characteristics

During the initial phase of the project, literature review was conducted by all partners. All collected documents were shared. Most relevant information regarding technology overview and reference solutions were discussed in work meetings (online). This section contains a selection of most relevant definitions and state of the art, based on literature review.

Definitions

Throughout this report, the following general terms have been applied:

For desalination processes, the feed water type is separated into categories expressed in ppm Total Dissolved Solids (TDS) [1]:

- 1) Seawater [20,000–50,000 ppm TDS];
- 2) Brackish water [3000-20,000 ppm TDS];
- 3) River water [500-3000 ppm TDS];
- 4) Pure water [below 500 ppm TDS];
- 5) Brine [above 50,000 ppm TDS]

It was agreed that for the NoBriner solution, the term **brine** covers also feed water below 50,000 ppm TDS (hypersaline concentrate), assuming that saline water from inland water sources is applied in a stand alone solution.

Desalination processes: By 2019, 99% of total desalinated water is produced with the following processes [2]:

- 1) Reverse Osmosis;
- 2) Multi-Stage Flash;
- 3) Multi-Effect Distillation;
- 4) Nanofiltration;
- 5) Electrodialysis/Electrodialysis Reversal;
- (6) Electrodeionization.

Furthermore, there are solar distillation and humidification-dehumidification processes existing, which are explained in the next subsection.

The desalination plant water recovery ratio (RR), is defined as the volumetric processing efficiency of the purification process – as applied for determining brine characteristics.

Zero liquid discharge: With spray evaporation, it is even possible to make a system, which evaporates 100 % of the water, a so-called zero discharge system. According to Dr. Yuan from



the Chinese Academy of Sciences, Chinese Research showed that crystallization of dissolved solid particles starts with a TDS concentration of about 50% [3]. When dissolved particles solidify (through crystallization), it is potentially possible to separate them from water.

Within this project, solidified dissolved solid particles are defined as salt.

Technology overview in relation to spray evaporation

In this section an overview of identified valuable aspects regarding the aimed spray evaporation solution by NoBriner are presented:

Jones et al. [2] reviewed the state of desalination and brine production. By 2019, 15,906 operational desalination plants were producing around 96 million m³/day of desalinated water for human use. A major challenge is the production of typically hypersaline concentrate – around 142 million m³/day. Its disposal is both costly and associated with negative environmental impacts.

Hoque et al [4] performed a study on innovative option for improving the performance of evaporation ponds based on the following background: Growing demand, concerns over droughts, over-allocation of surface water resources, and depletion of freshwater aquifers have all made desalination of brackish groundwater an increasingly important option for inland communities. However, these communities must find a means to dispose of the concentrated saline residual waste stream in an environmentally sound manner. Evaporation ponds are one of the primary options, but this technology has a large land requirement, which makes it costly. A concern for large facilities is that this technology is one of the few treatment methods that offers decreasing returns to scale due to increasing boundary layer resistance for larger ponds.

To enhance the performance of evaporation ponds, viable methods were identified from the literature: 1) fabric evaporators, 2) wetted boundary layer breakers, 3) salt-tolerant plants, and 4) droplet spraying. For the boundary layer breakers and for droplet spraying cost models were developed. Results indicate that both boundary layer breakers and spray technologies are cost-effective compared to a simple expansion of the pond area.

Xu et al. [5] concluded that membrane desalination technologies are typically associated with a much higher recovery rate than possible with thermal technologies. However, currently thermal processes using brine concentrator and crystallizer are considered mature industrial technologies to achieve zero liquid discharge or near zero liquid discharge of concentrate from low to high salinity; however, at high costs and intensive energy demand.

Consequently, zero liquid discharge – either through enhanced evaporation techniques in combination with evaporation ponds, or within thermal desalination processes (in industrial scale) – requires access to cheap and sustainable energy sources. Water desalination is typically applied in regions with high solar resources. There are plenty of possibilities for desalination using renewable energy including solar power. Numerous forms of plants are described in the literature. The idea of using the heat from the sun to distillate water from seawater is dominated by the following technologies (see Fig.1.1):



- a) Solar Distillation
- b) Humidification-Dehumidification
- c) Multiple Effect Distillation
- d) Multi Stage Flash Distillation (MSF) and MSF-Thermal Vapour Compression
- e) Membrane Distillation

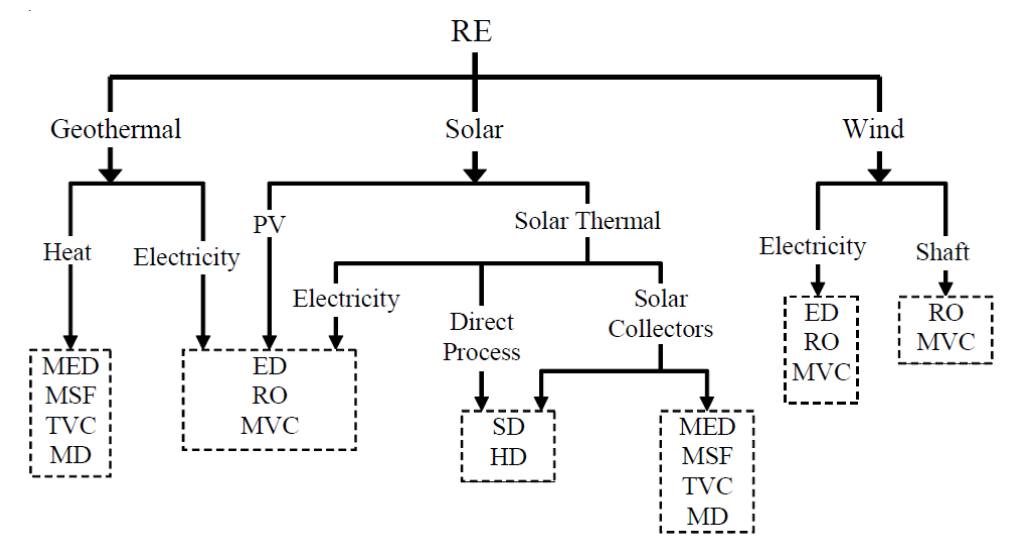


Fig.1.1.: Possible technological combinations of the main renewable energies and desalination methods [6].

It appears from the preliminary review that a) and b) solar distillation (SD) and Humidification-Dehumidification (HD) are the simplest technologies and relatively cheap compared to the other alternatives mentioned (c-e). However, they require much space and have therefore not been considered for large-scale applications. All technologies a-e are reasonably well described from a theoretic viewpoint and there are multiple descriptions of pilot installations.

Spray evaporation units (closed chambers) can be found for air humidification single and multiple stage air humidification dehumidification processes, where heat recovery is implemented in the condensation process (separation) of pure water. The following demonstration systems served as inspiration for investigations on spray evaporation in this project:

• Pilot plant installation of a solar desalination process by multiple-effect humidification at INRST-Tunisia [7]



Fig.1.2: Photo of the one-stage pilot plant constructed, including a spray evaporation unit [7].



 Discharge humidification and dehumidification at the Chinese Academy of Sciences, Institute of electrical Engineering. Possibilities for zero-liquid discharged were theoretically investigated by Johansen [8]. The system was later built – test runs resulted in high brine concentration. However, zero liquid discharge could not be achieved [9].

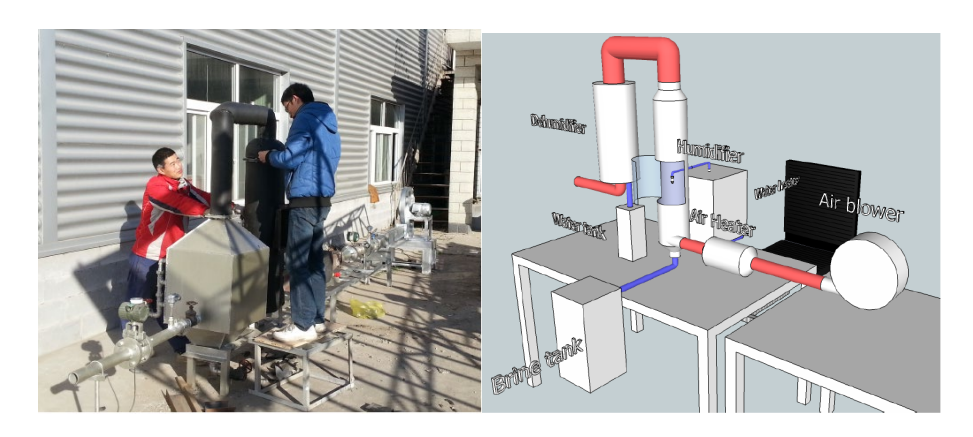


Fig.1.3.: Technical personal constructing part of the experimental setup (left); system setup showing the composition of components (right) [8].

• Multiple Effect Air Humidification Dehumidification system by Saltworks Technologies Inc. [10]

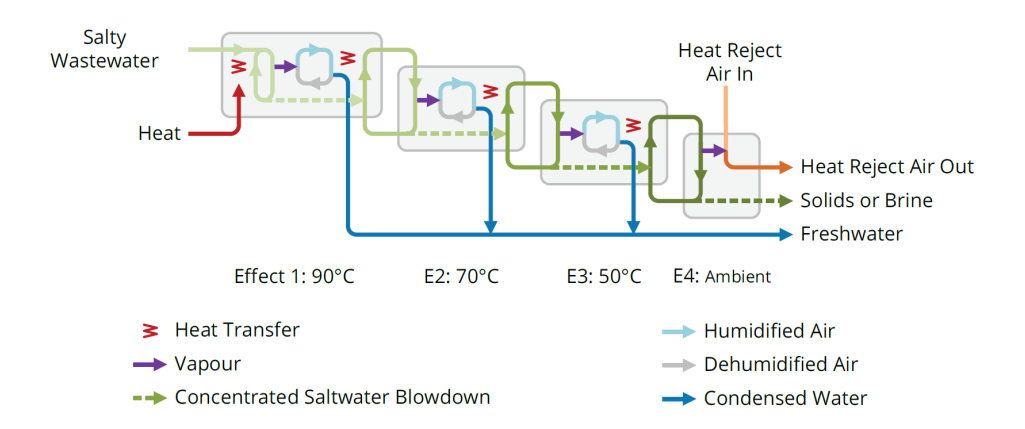


Fig.1.4: Operation scheme of multiple effect air humidification-dehumidification [10].

Furthermore, investigations on stand alone brine spray evaporation systems utilizing solar collectors have been performed:

- CFD modelling and analysis of a brine spray evaporation system integrated with solar collector [11]
- Design of a new spray-type seawater evaporator [12]



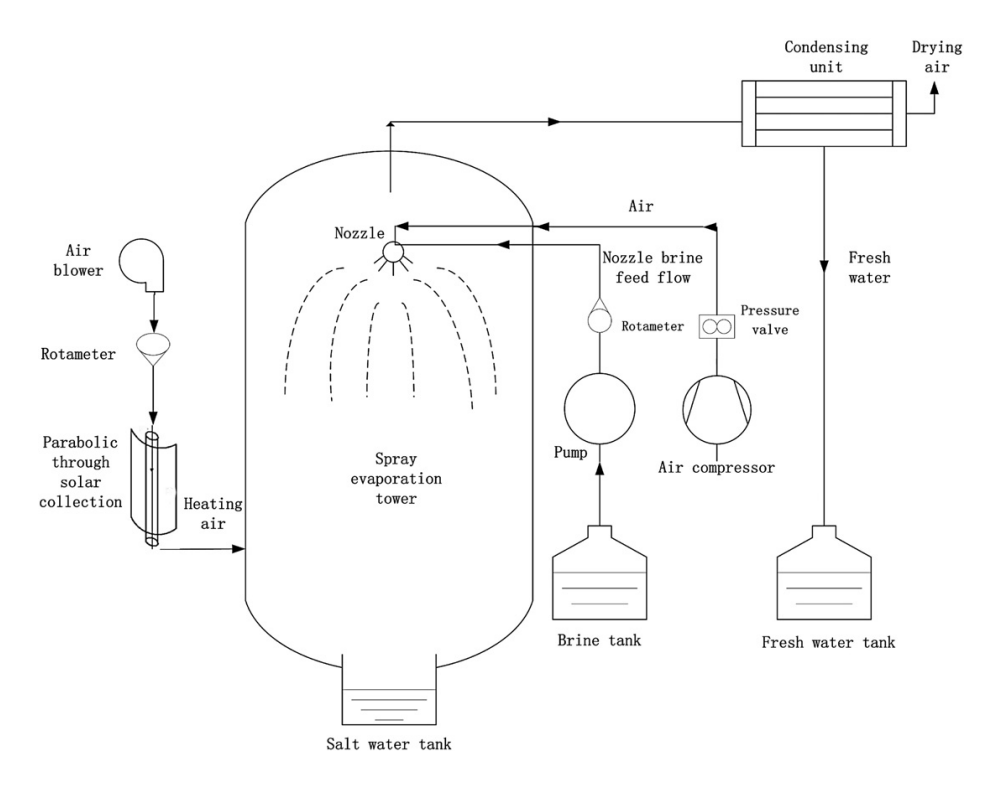


Fig.1.5: Schematic designs of a spray-type evaporator according to Xuening et al. [11]

In conclusion, humidification-dehumidification systems provide the possibility to reduce the volume of brine/ increase the concentration of hypersaline solutions significantly. It was found that only the system from the Canadian company Saltworks Technologies Inc. was capable of Zeroliquid discharge. This solution represents the absolute high end of HDH systems, both in terms of complexity and performance. Investigations on stand alone spray evaporation solutions showed satisfying performance for desalination – with limited production capacities. For example, the annual production of pure water with a unit designed by Kalogirou [12] was estimated with 11.2 m³ of desalinated water per square-meter solar collector area. A solution stand alone spray-type evaporation for zero-liquid discharge was not found in literature.



Brine characteristics

To determine "model brine" concentrations and their composition, analysis have been performed by DTU Miljø. Model concentrates have been determined in accordance with IMS Design 228.86.1.2, which utilizes databases on state of the art desalination technologies.

First, a saline water sample from an inland source in Kalobeyei (Kenya) - collected by Anne Sofie Larsen - was investigated. For concentration, a single-pass Reverse Osmosis desalination process was assumed. The corresponding recovery factor (pure water from brine) is 80%. Table 1.1 shows the obtained results.

Table 1.1: Model brine determination with saline water sample from Kolebeyei

| Composition | Initial | Concentrate | Concentrate meq | Model concentrate mg/L, ion balance validated in PhreeqC |
|-------------|---------|-------------|--------------------|--|
| рН | 7.8 | 8.44 | | 8.4 |
| Са | 13 | 65.2 | 3.26 | 65 |
| Mg | 5 | 25.1 | 2.066 | 25 |
| Na | 160 | 765 | 33.26 | 765 |
| К | 5 | 24.5 | 0.63 | |
| НСО3 | 230 | 1106 | 18.13 | 1106 |
| SO4 | 52 | 259.8 | 5.40 | 260 |
| CI | 90 | 444 | 12.51 | 445 |
| TDS | | | | 3001 |

Secondly, seawater properties from a reference database [13] have been investigated. For concentration, a two-pass Reverse Osmosis desalination process was assumed. The corresponding recovery factor (pure water from brine) is 90% after the second pass. Table 1.2 shows the obtained results.



Table 1.2: Model brine determination with reference seawater concentrations

| Composition | Initial | Concentrate | Model concentrate mg/L, ion balance validated in PhreeqC |
|-------------|---------|-------------|--|
| рН | 7 | 8.05 | 8.1 |
| Са | 410 | 819 | 820 |
| Mg | 1278 | 2554 | 2550 |
| Na | 10680 | 21045 | 21050 |
| К | 395 | 777 | 780 |
| HCO3 | | | 265 |
| SO4 | 2680 | 5341 | 5340 |
| CI | 19162 | 37835 | 37840 |
| TDS | | | 68800 |

The results show that standard seawater desalination with a recovery factor of 90% leads to a concentration of 7% of total dissolved solids (TDS) in the brine solution. NaCl is the dominating compound. Thus, using water with 7% NaCl is sufficiently accurate for experiments.

Dissolved bicarbonate and NaCl are the dominating compounds in the Kolebeyei water source. Low salt concentrations enable high recovery rates - considering 80% after a single pass - a TDS concentration of 0.3% in the brine solution is resulting. This means that for salt from this source a different application of potentially separated salt (NaCl 0,11%, HCO3 0,11%) is needed, compared to salt from seawater desalination. Furthermore, the salt output in a zero-liquid discharge process is corresponding to only 4.3% of those resulting when using brine from a typical seawater desalination process.

In conclusion, because NoBriner is aiming for a global technology solution, the use of model brine with NaCl concentrations in the range of 0.3 - 7% is valid for experimental tests.



2. Sustainable implementation

Social aspects on implementation

It is a core value in NoBriner to ensure that local communities benefit from the project in a sustainable manner. To ensure sustainable implementation - here defined as both environmentally, socially and financially sustainable - NoBriner wishes to define a methodology when working in the field. The main goal of developing a methodology is to determine any factors to be taken into consideration during the planning and execution of implementation by involving the parties from the very beginning. The focus here is on the social aspects that are a part of the implementation as well as the potential impact that the final solution may have on a community. The methodology is still a work in progress, but during the project period, the initial phases have been defined by analyzing field work that was done in Kakuma refugee camp in Kenya in July 2019. It is the hope of NoBriner to be able to share the results and methodology with other actors in the TechVelopment (technology for sustainable development) arena, so that through co-creation and collaboration, more and more sustainable solutions can be sustainably implemented to solve grand societal challenges while following the mantra of the Sustainable Development Goals of "leaving no one behind" and "reaching the furthest first".

Investigations in Kenya

As the pilot project takes place in Kakuma refugee camp and the surrounding local community, it is important to understand not just measurable aspects such as population, climate and water composition, but also the political background as well as the impact new livelihoods would have for the community. Because of the situation on the ground, especially social aspects on implementation are important, as the majority of the beneficiaries here have little to no sources of income. Kakuma refugee camp has existed since 1992 and today the camp along with Kalobeyei Integrated-Settlement hosts 196.666 registered refugees and asylum-seekers (UNHCR, 2020). The camp is in a "protracted situation", which UNHCR defines as "one in which refugees find themselves in a long-lasting and intractable state of limbo. Their lives may not be at risk, but their basic rights and essential economic, social and psychological needs remain unfulfilled after years in exile. A refugee in this situation is often unable to break free from enforced reliance on external assistance". As the camp has existed for so long, some refugees are born and raised in the camp and are now starting families of their own. Kalobeyei settlement is not in a protracted situation, and the refugees that settle here are closely connected to the local community of Kakuma, who reside just outside of the camp fences. The settlement has opened medical facilities and schools where both refugees and members of the local community are welcome. The surrounding community plays a significant role in our project, as our solution would physically be implemented here and not in the actual refugee camp.



The current situation is that the UN and Red Cross purchase safe drinking water from a third party and have it shipped to the refugee camp. The refugees receive the water directly while the local community in Kakuma actually purchase safe water from the camp. Our goal is to reverse this transaction, by making it possible for the local community to produce safe drinking water and sell it to the UN and Red Cross for distribution in the camp. The Red Cross however have long been looking to find local sources for water, but 8 out of 10 new boreholes reveal the groundwater to have too high salinity levels for this to be potable. We can help reverse the transaction by implementing the technical solution to manage the brine that would be the byproduct of the desalination of the groundwater. If implemented sustainably, our solution can help grant access to safe drinking water, help produce it responsibly and promote local job creation (also targeting SDG 6, 12 and 8).

Workshop

The first step of ensuring sustainable implementation is to ensure that the project and solution are targeting real issues. Up until the time of field work, NoBriner had been working on information from the Kenya Red Cross and a small Danish company called Little Dane. While this information has been the building blocks for us, it was important to verify the pilot project ourselves. A large part of the visit in the refugee camp was spent with this and the most significant outcome came from a workshop with participants representing Kenya Red Cross, UNHCR, refugees and local community members. Instead of presenting them with the project, we decided to start from the ground up. Even though we had language and cultural barriers, we managed to successfully communicate through cards with pictures on them. The main goal of the workshop was to establish the biggest issues facing the participants, to make sure our project was solving the right problem. The results from the workshop showed that access to safe water was the first priority. As one participant commented: "without water, we cannot do anything". With access to water, the community is able to grow crops as they would have water for irrigation and those crops could help feed livestock, leading to increased livelihoods in the entire area. The workshop is viewed as a success as we were able to verify the need for a solution that ensures safe, affordable drinking water.

The workshop also showed the value of including stakeholders from a variety of sources so as to show different aspects of the importance of access to water. Because of this, NoBriner wishes to use this way of investigating issues, wishes and solutions through inclusion of both organizations as well as local community members and refugees, to find a solution that is sustainable. By working this way, we hope to ensure sustainable implementation.

Methodology for sustainable implementation of technology

During the project NoBriner has defined the first two steps of a working methodology when planning for implementation on the ground:

1. Stakeholder identification and mapping. To ensure that all relevant actors' needs are met, it is important to first of all know who these actors are. By identifying all stakeholders from



- the beginning, the solution can be tailored to fit the right needs in the community and ensure domestication of the solution.
- 2. Verification and exploration of need or problem through co-creation methods. By using co-creation methods such as facilitating a workshop, the specific needs of a community can be verified and communicated from the actual beneficiaries. There are too many examples of "white elephants" (expensive high-tech solutions sent to development settings, but did not fit in or could not be used to its full extent ie. An electric well given to a village without electricity) and by understanding the community and its needs as well as resources will eliminate this risk.

The next step in the methodology will most likely include specifications of the solution by designing WITH the people on the ground.



3. Market exploration

Market overview

The phenomenon of desalination has been accompanying humankind throughout thousands of years starting with ancient Greek sailors evaporating seawater in order to quench their thirst over their endless seafaring. With freshwater sources becoming scarce in our recent past as well as present times, industrial desalination has become a standard practice to obtain and secure fresh water for millions (if not billions) of people around the globe. Current estimates state that there are roughly 16.000 desalination plants in the world providing about 95 million m³ desalinated water every day [14], utilizing various technologies to do so.

Regardless of the used methods, a significant factor in desalination plants feasibility, sustainability, and overall impact has been ignored to an alarming degree. The super saline residue left behind by desalination processes – also known as brine- poses a considerable threat to the environment it comes in contact with. While the toxicity of brine is known, it's handling is not matching it's destructive potential, as most desalination plants have chosen to discharge brine back to the source of saline water, prompting several negative effects to present themselves on both the short-, and long run. The consequential damage can reveal itself in various fields ranging from economic perspectives to ecologic eradication, not to mention location specific problems such as Cape Town where careless brine discharge into the city's sewer system has corroded it's pipes and is now posing serious consequences to its inhabitants. To emphasize the weight of the issue the United Nations have issued a warning on the alarming levels of brine discharge amounting to a 142 million m³ daily discharge.

On the other hand, salt is one of the most important raw materials used in a wide, and ever increasing number of fields from the food industry to state-of-the-art nuclear reactors. Thus, theoretically it would seem that brine is the key factor for closing the loop in not just the desalination industry but several industries relying on a steady supply of salt in large quantities.

However, investigations into the fields of brine and salt reveal that the picture is not as clear as it may seem at first glance. Due to various technologies, treatments, water sources and geographies the composition of brine varies tremendously on a wide spectrum of chemicals, and thus the chemical composition of salt extracted will be case-specific. Based on the outcome in turn, mounts an even higher number of potential applications.

The evident conundrum can be solved in a number of ways depending on the point of origin. From the process-oriented viewpoint, one could look at the desired use for salt such as salt used for the detergent industry, and then "reverse engineer" the process all the way to finding the desired brine profile for the specific purpose. On the other hand one could also focus on the input brine instead of the output salt, which results in a more generic approach. Both viewpoints carry several implications for the business operation aspects of the desired solution. Looking from the outcome perspective, since the desired industry is decided, emphasis is put on thorough geographical scouting to find brine with the right characteristics including pre-, and post-treatment and hopefully



not too far from the buyer. Whereas looking from the input perspective geographical scouting becomes less of importance along with technological aspects of the desalination plant. However, in this case the creation of the right product becomes crucial.

Potential applications cases

NoBriner has utilized so far the latter approach for a number of reasons. The companies' solution aims to be a more generally applicable resolution to inefficiencies in brine management, therefore a flexibility in selecting projects is highly desirable. Due to the currently practiced business model, NoBriner also relies on the variety of its solutions in order to provide a product for the benefit of the local community and thus lower transportation-related costs, as well as increase its appeal as a business opportunity for the local stakeholders. To ease the task of creating the right product the firm plans to enhance its knowledge using co-creation processes and work together with local stakeholders to custom tailor a solution.

These processes the company has been engaging has so far proven to be successful in terms of local interest in the cases it has been contextualized, and thus gives NoBriner reason to continue the exploration. At this stage the main attempts for product creation have also put an emphasis on the low technology level required to harness the product, as the firms' partners are predominantly located in underdeveloped, or even off-grid locations.

Naturally when mentioning the word salt, one's mind associates it with it's consumption purposes, which is also the easiest form of a salt product available for the company. The issue arises however when the question of quality and quantity is discussed. The main assumption is that salt harvested from brine will be of the required quality. If that assumption holds true, NoBriner can simply sell its product to the world market as a commodity. However, during the investigation into compositions of brine and salt has shown that consumption grade salt is harder to achieve than initially expected.

The first solution that has been explored is in the context of the project NoBriner has been involved with, and is located in Kakuma, Kenya, and is namely the refugee camp operated by the United Nations (UN). Trying to solve the issue of sustainable desalination in order for the inhabitants of the camp to gain access to drinking water is just one of the many challenges faced on a daily basis by operatives. Housing the camps' nearly 200,000 inhabitants inevitably poses housing issues. A solution to this problem can very well prove to be brine, in the form of providing enough salt for construction purposes. Inspired by Eric Geboers' study in 2015 [15] on viability of using salt for construction in arid regions, NoBriner sees great potential in creating salt bricks out of salt from brine. A solution that both creates sustainable desalination and therefore secures a sustainable source of fresh water, but also creates a sustainably sourced material for the construction industry.

Along similar principles of using salt as a coating or building material several options are at NoBriner's disposal. As the California-based company Emerging Objects has showcased, salt could prove to be a material fit for 3D printing [16]. Such a novel use could potentially secure



rather high profit margins with relatively low investment capital requirement. Although the technology applied in this specific use is unknown to NoBriner at this point, with proper research this commercialization strategy offers tremendous potential.

Another option in relation to the difficult and subpar living conditions of the camp residents is to turn the companies' attention towards hygiene. Not just in the sense of personal hygiene but also the newly secured water source also need to be cleansed of any contaminants. The main use of salt in an industrial context is to produce chlorine and caustic soda which are then -among other uses, utilized in the detergent industry to create a wide variety of cleaning products. By supplying the necessary raw material, NoBriner is able to provide responsibly sourced product and thus also push detergents towards a more sustainable future. An alternative use in the same domain could be to partner with a company called Aqua Research that provides a portable water purifier that only needs salt to produce a purifying agent [17].

According to newer studies in the field of reject brine treatment, brine —or salt as the end product-could be an agent of decarbonization and utilize the waste CO2 emitted from power plants, or other industrial buildings [18]. As with most of the previous methods, actual feasibility studies will have to be conducted, as it is not known how refined is the technology behind such a solution. However, this viability could provide a solution to several hardware requirements of NoBriners' brine treatment machine, due to the necessity of being close to a power plant and thus having access to power that can fuel the machine.

Due to the method of processing salt after separating it from brine (NoBriner planned to utilize local workforce), the firms' product provides marketing possibilities to its buyers. Combining the CSR and sustainability value of the salt with the possible applications in detergents, approaching companies working with manufacturing cosmetics products seems to be a trivial direction. As such NoBriner has been already approached by French high-end brand l'Occitane en Provance, as a potential supplier of raw materials.

One of the most critical aspects of the operation of NoBriners' hardware is the presence of a power source –just like with many other machinery. The world is in a dire need for sustainable energy. In a desperate attempt to move from energy provided by burning fossil fuels, nuclear power is becoming a more and more viable substitute. The relevancy of NoBriner in this field could prove to be more than one can think of at first thought. Salt, or molten salt has already proven its capabilities to store energy, and Moltex Energy Ltd. has developed a Stable Salt Reactor (SSR) that uses a fuel consisting of two-third table salt. Sustainably sourced table salt in this scenario could prove to be an agent of providing clean energy, and in turn be the key for the future of sustainably sourced energy.

Although mostly theoretical uses of brine, or salt has been introduced in this section, the aim was to show the diversity of applications and their respective value drivers, and thus to provide an outlook on the place NoBriner can take in different value chains of different industries. The next step for the company is then as follows: to find the most commercially viable path and organize its processes towards that path in order to be able to finance further alternative uses and provide groundbreaking solutions to replace unsustainable salt in various industries. The ultimate



goal/vision of the company is to eliminate unsustainable desalination in the world, and through salt bring forth a new way of thinking in the business world; prosperity for all, without exploitation or damage.



4. Development of simulation models for NoBriner's spray evaporation unit

Pure water spray evaporation model (Python)

The pure water spray evaporation model calculates and simulates the evaporation process of a pure water droplet heated by surrounded warm air. The water droplets are sprayed into the plug pipe while the warm airflow is also blown in at the same time. The model diagram can be seen in Fig. 4.1. The water droplet will be evaporated into water vapor during the stay in the pipe and the air humidity will increase. At a certain time, either a water droplet is fully evaporated or the air relative humidity reaches 100%, then the water, water vapor and air will keep the same status afterwards. The water droplet can be sprayed by a nebulizer for example a nozzle into a pipe device.

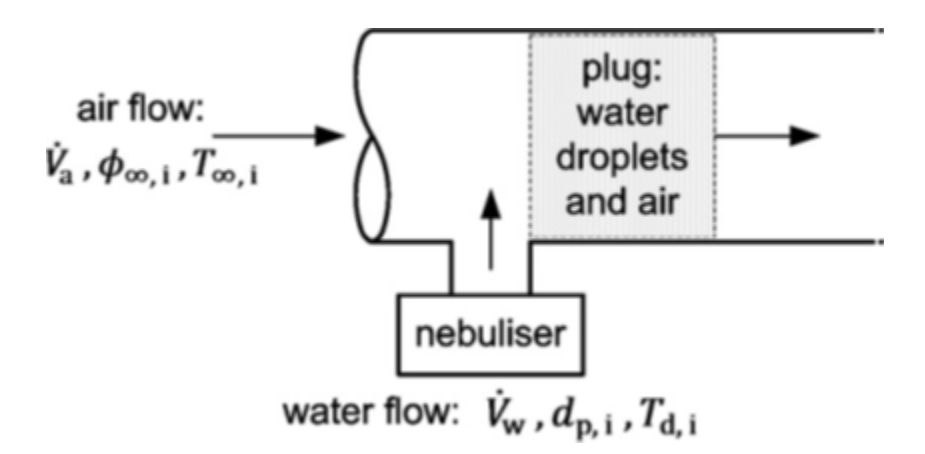


Fig. 4.1. Evaporation diagram [19].

The evaporation process is described by a set of four differential equations [19].

The first differential equation determines the water droplet size.

$$\frac{dd_p}{dt} = \frac{4D_w M_w}{\rho_w d_p R_u} \left(\frac{p_\infty}{T_\infty} - \frac{p_d}{T_d}\right) C_m \tag{1}$$

The second equation determines the temperature of the droplet.



$$\frac{dT_d}{dt} = -\frac{12}{\rho_w d_p^2 C_{p,w}} \left[\frac{D_w M_w h_w}{R_u} \left(\frac{p_d}{T_d} - \frac{p_\infty}{T_\infty} \right) C_m + k_f C_h \left(T_d - T_\infty \right) \right] \tag{2}$$

The third differential equation determines the partial pressure of water vapor in the surrounding air.

$$\frac{dp_{\infty}}{dt} = -\left(\frac{\rho_w \pi d_p^2 N_d R_u T_{\infty}}{2M_w}\right) \frac{dd_p}{dt} \tag{3}$$

And the fourth equation determines the temperature in the surrounding air.

$$\frac{dT_{\infty}}{dt} = \frac{\pi d_p N_d (T_{\infty} - T_d)}{2\rho_{\infty} C_{p,\infty}} \left[\rho_w d_p \frac{dd_p}{dt} C_{p,wv} - 4k_f C_h \right]$$

(4)

The four dependent variables using in the above differential equations are droplet diameter assuming spherical droplets dp [m], droplet temperature Td [K], partial pressure of water vapor in the surrounding air p1 [Pa] and surrounding humid air temperature T∞[K].

The nomenclature of the four differential equations can be seen in Table 4.1 [19].



| Symbol | Property/description |
|-----------------------|--|
| Ch | Correction factor based on Knudsen number, for heat transfer |
| C_m | Correction factor based on Knudsen number, for mass transfer |
| $C_{p,\infty}$ | Specific heat capacity of the surrounding humid air (I/kg K) |
| $C_{p,w}$ | Specific heat capacity of water (J/kg K) |
| $C_{p,wv}$ | Specific heat capacity of water vapour (J/kg K) |
| d_p | Droplet diameter (m), assuming spherical droplet |
| $d_{p,i}$ | Initial droplet diameter (m) |
| D_{w} | Diffusion coefficient for water vapour in air (m²/s) |
| h_w | Latent heat of vaporisation of water (J/kg) |
| k_f | Thermal conductivity of the humid air (W/m K) |
| Kn | Knudsen number (= $2\lambda/d_p$) |
| $M_{\rm w}$ | Molar mass of water = 18.015 (kg/kmol) |
| N_d | Droplet number concentration (/m3) represents the ratio of water |
| | to air in the system and is equal to $6\dot{V}_w/\pi d_p^3\dot{V}_a$ |
| p_d | Partial pressure of water vapour at the curved droplet surface (Pa) |
| p_{∞} | Partial pressure of water vapour in the surrounding air (Pa) |
| $p_{\infty,i}$ | Initial partial pressure of water vapour in the surrounding air (Pa) |
| p_o | Ambient total pressure (Pa) |
| p_s | Saturation pressure of water vapour above a flat surface (Pa) |
| R_u | The universal gas constant = 8314.47 (J/k mol K) |
| t | Time (s) |
| T_{∞} | Temperature of surrounding humid air (K) |
| $T_{\infty,i}$ | Initial temperature of surrounding humid air (K) |
| T_d | Temperature of droplets and of humid air at the droplet surface (K) |
| $T_{d,i}$ | Initial temperature of droplets and of humid air at the droplet |
| | surfaces (K) |
| \dot{V}_a | Volume flow rate of air (m ³ /s) |
| $\dot{V}_{\rm w}$ | Volume flow rate of water (m ³ /s) |
| α_h | Thermal accommodation coefficient |
| α_m | Mass accommodation coefficient |
| ϕ_{∞} | Relative humidity (RH) of the surrounding air |
| $\phi_{\infty,i}$ | Initial relative humidity (RH) of the surrounding air |
| λ | Mean free path of gas surrounding droplet (m) |
| $ ho_{\infty}$ | Density of the surrounding humid air (kg/m ³) |
| $ ho_{ m w}$ | Density of water (kg/m ³) |
| σ_{w} | Surface tension of water (N/m) |

Table 4.1. Nomenclature of the differential equations [19]

The python code of the spray evaporation model is developed based on the original work of Jakob Brinkø Berg [8]. The functionality of the model is extended and improved. For example the program developed the stopping conditions for calculations and outputs tabulate results with varying input parameters for sensitivity analysis. The source code can be found in the appendix.

The logic flow chart of the program is shown in Fig. 4.2.



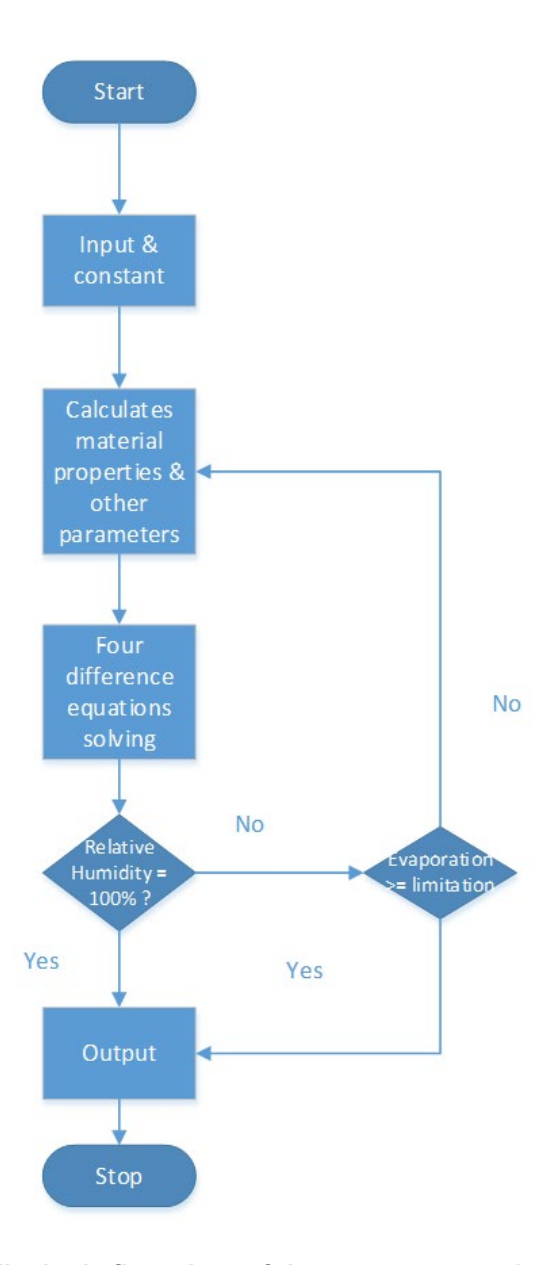


Fig. 4.2. The logic flow chart of the spray evaporation model.

The program starts with the input from users, see Fig. 4.3. All the parameters with square brackets can be offered with multi values separated by a comma. The program will output a summary table with all parameters varied. The evaporated threshold determines the evaporation limitation of the water droplet, which will stop the calculation. The simulation time determines the total calculation time and the time step determines the total calculation steps in the whole simulation time.



```
# Initial droplet diameter [um]
DropletDiameterInput = [100,200]
# Initial temperature of the droplet [°C]:
DropletTemperatureInput = [30,40]
# Initial temperature of the surrounding air [°C]:
AirTemperatureInput = [50,60,70,80]
# Mass flow rate of air [kg/h]:
AirMassFlowrateInput = [50]
# Water volume flowrate [liter/h]:
WaterFlowInput = [1]
# Initial relative humidity of surrounding air [%]:
RelativeHumidityInput = [5.3]
# Mass evaporated threhold [%]: If MET is X, set X-0.1 below.
MET=89.9
# Simulation time [s]: if no results, try a longer simulation time
Time = 5
# Timesteps of simulation time:
Timestep = Time*500
```

Fig. 4.3: Inputs from users.

The constants are defined in Fig. 4.4 and the material parameters are calculated in Fig. 4.5:

```
# The latent heat of evaporation of water [k]/kg]:

h_w = 2257

# The molar mass of water [kg/kmol]:

M_w = 18.015

# The molar mass of dry air [kg/kmol]:

M_a = 28.97

# The ambiant pressure [Pa]:
p_0 = 101325

# The universal gas constant []/(kmol*K)]:

R_u = 8314.47

# The thermal accmodation coefficient (1999, Raymond A. Shaw et al):
alpha_h = 0.7

# The mass accmodation coefficient (undetermined between three orders of magnitude in the literature (2004, P. Davidovits):
alpha_m = 0.1

# The mean free path of the surrounding air [m]
lambdas = 70*10**(-9)

# Corpresibility factor for air at 1 atm:
2 = 1
```

Fig. 4.4: Program constants



```
***Material properties**

**Saturation pressure calculation (2007, P.T. Tsilingiris) [Pa]: p.s = (0.7073 - 2.708*10**(-2)*(x[3]-273.15) * 4.5609*10**(-3)*(x[3]-273.15)**3 + 1.0347*10**(-6)*(x[3]-273.15)**4 * 100**3 * 8.81ative hundity pit inf = (x[2]/p_3)*100** * Specific heat capacity of surrounding air <a href="http://mae.engineeringtoolbox.com/hundity-ratio-air-d_686.html">http://mae.engineeringtoolbox.com/hundity-ratio-air-d_686.html</a> [k3/(kg*K]: C.p. inf = 3.01 + 1.68*(0.02100**(pit_inf)/p.0 - pht_inf)))

**Specific heat capacity of water (203.15 K) [k1/(kg*K]: C.p. inf = 3.01 + 1.68*(0.02100**(pit_inf)/p.0 - pht_inf)))

**Specific heat capacity of water vapour (300 K) [k3/(kg*K]: C.p. inf = 3.01 + 1.68*(0.02100**(-10)*10**(0.0100**)) [k1/(kg*K]: C.p. inf = 3.01 + 1.68*(0.02100**(-10)*10**(0.0100**)) [k1/(kg*K]: C.p. inf = 3.01 + 1.68*(0.02100**) [k1/(kg*K]: C.p. inf = 3.01 + 1.68*(0.02100**)] [k1/(kg*K]: C.p. inf = 3.01 + 1.68*(0.02100**) [k1/(kg*K]: C.p. inf = 3.01 + 1.68*(0.02100**)] [k1/(kg*K]: C.p. inf = 3.01 + 1.68*(0.02100**)] [k1/(kg*K]: C.p. inf = 3.0100**) [k1/(kg*K]: C.p. inf = 3.010**) [k1/(kg*K]: C.p. inf = 3.010**] [k1/(kg*K]: C.p. inf = 3.01
```

Fig. 4.5: Material properties calculation.

Then the program will calculate the four differential equations. Of course, there are inner iteration calculations in solving the differential equation set. When the calculation converges, the relative humidity (RH) of the outlet air will be checked first. If the RH reaches 100%, the results will be output. Otherwise, the mass evaporation rate will be checked and the results will be output until the mass evaporation rate reaches the limitation.

The results will be output as a summary table shown in Fig. 4.6. The input parameters are shown in the left hand part while the results are shown in the right hand side. It can be seen from the figure that the calculation stops at either RHOut reach 100% or MassEvaporated reach 90%. But there are still six cases with RHOut less than 100% and MassEvaporated less than 90%, which indicates a longer simulation period is required. Therefore, the time should be set longer in the input zone. The output results can be seen in Fig. 4.7 when the time period is set to 20 s.

| DiameterIn[um] | DropletTempIn[°C] | AirTempIn[°C] | AirFlow[kg/h] | WaterFlow[1/h] | RHIn[%] | ConverageTime[s] | DiameterOut[um] | DropletTempOut[°C] | RHOut[%] | AirTempOut[°C] | MassEvaporated[%] |
|----------------|-------------------|---------------|---------------|----------------|---------|------------------|-----------------|--------------------|----------|----------------|-------------------|
| 100 | 30 | 50 | 50 | 1 | 5.3 | 4.49 | 74.57 | 24.78 | 100 | 24.78 | 58 |
| 100 | 30 | 60 | 50 | 1 | 5.3 | 4.25 | 65.75 | 28.87 | 100 | 28.87 | 72 |
| 100 | 30 | 70 | 50 | 1 | 5.3 | 4.28 | 53.57 | 32.97 | 100 | 32.97 | 85 |
| 100 | 30 | 80 | 50 | 1 | 5.3 | 0.87 | 46.66 | 40.14 | 80 | 40.16 | 90 |
| 100 | 40 | 50 | 50 | 1 | 5.3 | 4.48 | 73.85 | 25.02 | 100 | 25.02 | 60 |
| 100 | 40 | 60 | 50 | 1 | 5.3 | 4.27 | 64.76 | 29.07 | 100 | 29.07 | 73 |
| 100 | 40 | 70 | 50 | 1 | 5.3 | 4.35 | 51.99 | 33.14 | 100 | 33.14 | 86 |
| 100 | 40 | 80 | 50 | 1 | 5.3 | 0.79 | 46.6 | 40.81 | 77 | 40.84 | 90 |
| 200 | 30 | 50 | 50 | 1 | 5.3 | 5 | 153.89 | 26.42 | 85 | 26.43 | 54 |
| 200 | 30 | 60 | 50 | 1 | 5.3 | 5 | 137.1 | 30.38 | 87 | 30.39 | 68 |
| 200 | 30 | 70 | 50 | 1 | 5.3 | 5 | 115.02 | 34.41 | 89 | 34.42 | 81 |
| 200 | 30 | 80 | 50 | 1 | 5.3 | 3.44 | 93.27 | 40.13 | 80 | 40.16 | 90 |
| 200 | 40 | 50 | 50 | 1 | 5.3 | 5 | 152.55 | 26.66 | 85 | 26.66 | 55 |
| 200 | 40 | 60 | 50 | 1 | 5.3 | 5 | 135.32 | 30.59 | 87 | 30.6 | 69 |
| 200 | 40 | 70 | 50 | 1 | 5.3 | 5 | 112.44 | 34.61 | 89 | 34.62 | 82 |
| 200 | 40 | 80 | 50 | 1 | 5.3 | 3.13 | 93.16 | 40.81 | 77 | 40.84 | 90 |

Fig. 4.6: Output results in a summary table with 5 s simulation time.



| DiameterIn[um] | DropletTempIn[°C] | AirTempIn[°C] | AirFlow[kg/h] | WaterFlow[1/h] | RHIn[%] | ConverageTime[s] | DiameterOut[um] | DropletTempOut[°C] | RHOut[%] | AirTempOut[°C] | MassEvaporated[%] |
|----------------|-------------------|---------------|---------------|----------------|---------|------------------|-----------------|--------------------|----------|----------------|-------------------|
| 100 | 30 | 50 | 50 | 1 | 5.3 | 4.49 | 74.57 | 24.78 | 100 | 24.78 | 58 |
| 100 | 30 | 60 | 50 | 1 | 5.3 | 4.25 | 65.75 | 28.87 | 100 | 28.87 | 72 |
| 100 | 30 | 70 | 50 | 1 | 5.3 | 4.28 | 53.57 | 32.97 | 100 | 32.97 | 85 |
| 100 | 30 | 80 | 50 | 1 | 5.3 | 0.87 | 46.63 | 40.13 | 80 | 40.16 | 90 |
| 100 | 40 | 50 | 50 | 1 | 5.3 | 4.48 | 73.85 | 25.02 | 100 | 25.02 | 60 |
| 100 | 40 | 60 | 50 | 1 | 5.3 | 4.27 | 64.76 | 29.07 | 100 | 29.07 | 73 |
| 100 | 40 | 70 | 50 | 1 | 5.3 | 4.35 | 51.99 | 33.14 | 100 | 33.14 | 86 |
| 100 | 40 | 80 | 50 | 1 | 5.3 | 0.79 | 46.6 | 40.81 | 77 | 40.84 | 90 |
| 200 | 30 | 50 | 50 | 1 | 5.3 | 17.78 | 149.14 | 24.78 | 100 | 24.78 | 58 |
| 200 | 30 | 60 | 50 | 1 | 5.3 | 16.83 | 131.49 | 28.87 | 100 | 28.87 | 72 |
| 200 | 30 | 70 | 50 | 1 | 5.3 | 16.9 | 107.14 | 32.97 | 100 | 32.97 | 85 |
| 200 | 30 | 80 | 50 | 1 | 5.3 | 3.45 | 93.26 | 40.13 | 80 | 40.16 | 90 |
| 200 | 40 | 50 | 50 | 1 | 5.3 | 17.74 | 147.7 | 25.02 | 100 | 25.02 | 60 |
| 200 | 40 | 60 | 50 | 1 | 5.3 | 16.9 | 129.52 | 29.07 | 100 | 29.07 | 73 |
| 200 | 40 | 70 | 50 | 1 | 5.3 | 17.19 | 103.98 | 33.14 | 100 | 33.14 | 86 |
| 200 | 40 | 80 | 50 | 1 | 5.3 | 3.13 | 93.17 | 40.81 | 77 | 40.84 | 90 |

Fig. 4.7: Output results in a summary table with 20 s simulation time.

The water spray model was validated by comparing the output results in the paper [19].

Brine spray evaporation model (Python)

The water spray evaporation model was further developed into the brine droplet model. It is a new version of the simulation model with the frame restructured. The main feature is that it calculates the dynamic brine solution properties, which means the salt concentration and saline solution properties updated at each time step.

The usage of the model is also different from the water evaporation model. It can only simulate the evaporation process from the initial concentration condition to the saturated condition. The model cannot simulate the salt separation process after the solution is saturated. Therefore, a maximum concentration limit was set that stops the process. The maximum concentration will be calculated according to the droplet temperature internally at each time step. If there is no limitation of the maximum salt concentration, the model will give very small changes in droplet diameters around the maximum concentration. Another situation is that if the initial concentration is small, the droplet solution may not reach the saturated condition and the salt concentration slowly increases. In this case, the set time will be all used and the droplet and air temperature are low and the air has no energy to evaporate the droplet quickly.

Another feature for the model is that an option for two boundary conditions are added in the input zone. The default boundary condition recommended by literature is adiabatic but the isothermal condition is more reasonable when the hot air flow rate is high. In reality, the boundary condition is between the two conditions.

The logic flow chart for brine spray evaporation model can be seen in Fig. 4.8. Compared to the logic flow chart of water spray evaporation model in Figure 3, the internal updates of material properties is indicated by a closed loop between material properties calculation and the four differential equation solving. In addition, a new decision condition of maximum salt concentration is added.

The input, constants, material properties calculation and the results output example can be seen in the Figures 4.9 to 4.12.

The brine spray evaporation model has not been validated by any experiments or literature results.



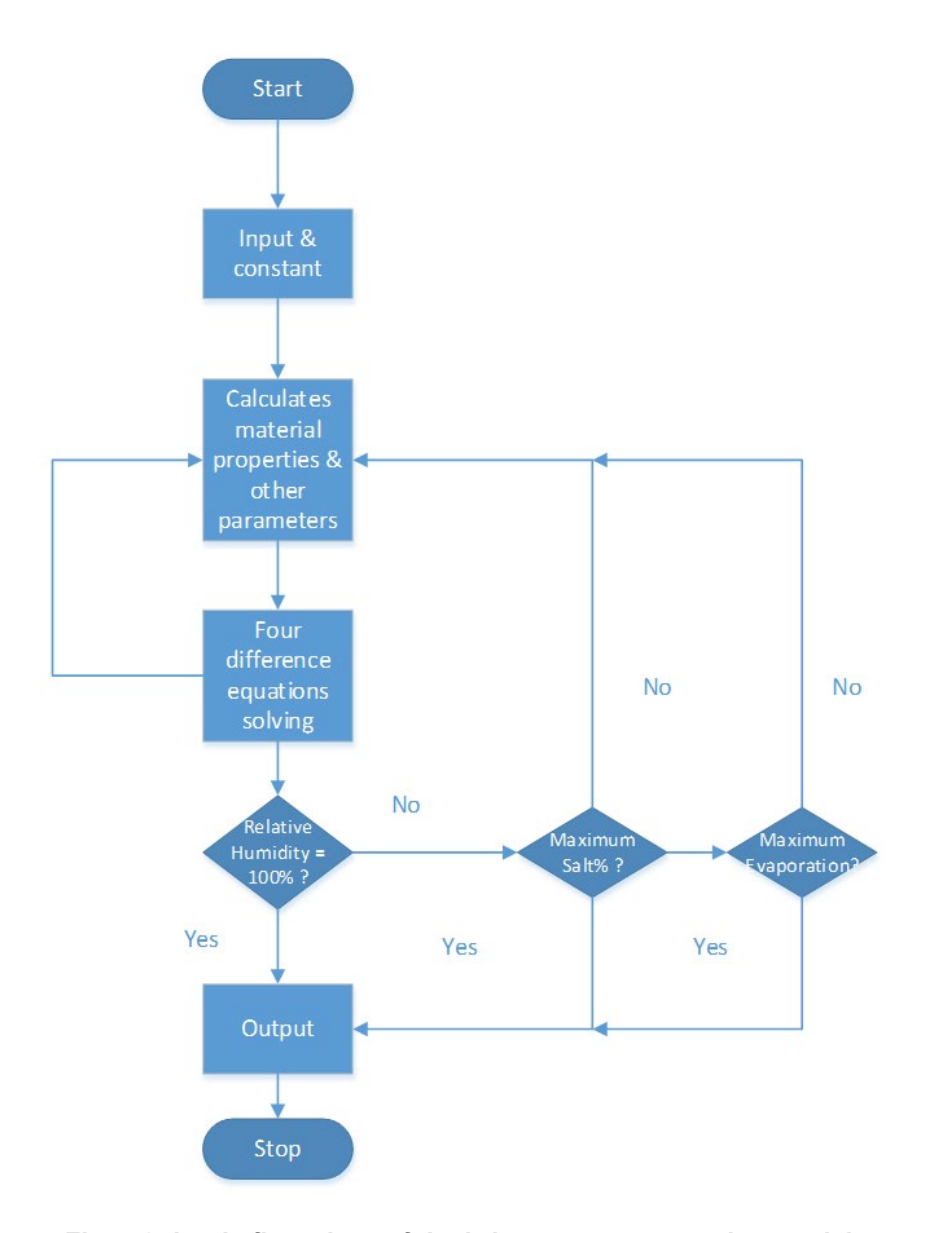


Fig. 4.8: Logic flow chart of the brine spray evaporation model.



```
# Initial droplet diameter [um]
DropletDiameterInput = [100]
# Initial temperature of the droplet [°C]:
DropletTemperatureInput = [30]
# Initial temperature of the surrounding air [°C]:
AirTemperatureInput = [60]
# Mass flow rate of air [kg/h]:
AirMassFlowrateInput = [50]
# Water volume flowrate [liter/h]:
WaterFlowInput = [1]
# Initial relative humidity of surrounding air [%]:
RelativeHumidityInput = [5.3]
# Brine concentration [%]:
NaC1 = 7
# Mass evaporated threhold [%]: If MET is X, set X-0.1 below.
MET=99.9
# Simulation time [s]: if no results, try a longer simulation time
# Boundary Condition 0 for adiabatic and 1 for isothermal
BouCond = 0
```

Fig. 4.9: Input parameters of brine spray evaporation model

```
# The latent heat of evaporation of water [k]/kg]:
h_w = 2257
# The molar mass of Brine [kg/kmol]: https://pubchem.ncbi.nlm.nih.gov/compound/Brine
M_w = 76.46
# The molar mass of dry air [kg/kmol]:
M_a = 28.97
# The ambiant pressure [Pa]:
p_0 = 101325
# The universal gas constant [J/(kmol*K)]:
R_u = 8314.47
# The thermal accmodation coefficient (1999, Raymond A. Shaw et al):
alpha_h = 0.7
# The mass accmodation coefficient (undetermined between three orders of magnitude in the literature (2004, P. Davidovits):
alpha_m = 0.1
# The mean free path of the surrounding air [m]
lambdas = 70*10**(-9)
# Corpresibility factor for air at 1 atm:
Z = 1
```

Fig. 4.10: Constant parameters of brine spray evaporation model



Fig. 4.11: Material properties calculation of brine spray evaporation model

| DiameterIn[um] | DropletTempIn[°C] | AirTempIn[°C] | AirFlow[kg/h] | WaterFlow[1/h] | RHIn[%] | Time[s] | DiameterOut[um] | DropletTempOut[°C] | RHOut[%] | AirTempOut[°C] | MassEvap[%] | Salt[%] |
|----------------|-------------------|---------------|---------------|----------------|---------|---------|-----------------|--------------------|----------|----------------|-------------|---------|
| 100 | 30 | 50 | 50 | 1 | 5.3 | 2 | 66.95 | 17 | 83 | 17 | 68 | 21.65 |
| 100 | 30 | 60 | 50 | 1 | 5.3 | 0.6 | 62.51 | 24.11 | 67 | 24.13 | 73 | 26.23 |
| 100 | 30 | 70 | 50 | 1 | 5.3 | 0.2 | 62.13 | 33.68 | 48 | 33.78 | 74 | 26.4 |
| 100 | 30 | 80 | 50 | 1 | 5.3 | 0.1 | 62.08 | 43.53 | 37 | 43.77 | 74 | 26.6 |
| 100 | 40 | 50 | 50 | 1 | 5.3 | 2 | 66.08 | 17.21 | 82 | 17.21 | 69 | 22.23 |
| 100 | 40 | 60 | 50 | 1 | 5.3 | 0.5 | 62.3 | 24.72 | 64 | 24.75 | 73 | 26.24 |
| 100 | 40 | 70 | 50 | 1 | 5.3 | 0.2 | 61.75 | 34.2 | 47 | 34.31 | 74 | 26.41 |
| 100 | 40 | 80 | 50 | 1 | 5.3 | 0.1 | 61.15 | 43.78 | 37 | 44.02 | 75 | 26.61 |
| 200 | 30 | 50 | 50 | 1 | 5.3 | 2 | 142.81 | 19.9 | 64 | 19.93 | 61 | 18.15 |
| 200 | 30 | 60 | 50 | 1 | 5.3 | 2 | 126.46 | 24.46 | 65 | 24.49 | 72 | 25.44 |
| 200 | 30 | 70 | 50 | 1 | 5.3 | 0.9 | 124.82 | 33.76 | 48 | 33.86 | 74 | 26.4 |
| 200 | 30 | 80 | 50 | 1 | 5.3 | 0.4 | 124.39 | 43.48 | 37 | 43.72 | 74 | 26.6 |
| 200 | 40 | 50 | 50 | 1 | 5.3 | 2 | 141.2 | 20.08 | 63 | 20.11 | 62 | 18.55 |
| 200 | 40 | 60 | 50 | 1 | 5.3 | 2 | 124.57 | 24.68 | 65 | 24.71 | 73 | 26.24 |
| 200 | 40 | 70 | 50 | 1 | 5.3 | 0.8 | 124.41 | 34.37 | 46 | 34.48 | 74 | 26.41 |
| 200 | 40 | 80 | 50 | 1 | 5.3 | 0.4 | 123.97 | 44.08 | 36 | 44.33 | 74 | 26.61 |

Fig. 4.12: Results output example of brine spray evaporation model



Parametric study of droplet evaporation

The key parameter for spray evaporation process the droplet evaporation time - sufficient water must be evaporated within the reaction chamber in order to enable brine crystallization (50%< according to [3]).

As a basic scenario brine from seawater desalination (section 1) with 7% of TDS was chosen. Water evaporation of 90% of the brine mass was assumed - corresponding to a final TDS concentration of 70%, in which case salt should be crystalline. For the first assessment a droplet remaining time in the spray evaporator of 10 second was assumed.

To investigate how air must be conditioned prior spray evaporation, a parametric study was performed - the pure water model was applied for sensitivity analysis of required temperatures with variation of initial droplet diameter and air flow. Droplet diameters in the range of 100-500 micrometer were chosen as expected practical distribution - utilizing air atomizing nozzles (more information see section 5). An absolute air humidity of 6.5 g water/kg dry air was applied - a typical value for a summer day in a dry region. The pure water model was chosen because of its proofed plausibility and conservative calculation method - since adiabatic conditions are considered and slower evaporation rates can be expected in comparison to brine.

Calculation results are presented in Fig. 4.13. The air flow range was tested systematically. Air flow rates in the range of 70-150 m³/h for a spraying rate of 1 kg brine/h were found to be practical. With the chosen conditions, an air temperature of 40 °C would be only sufficient if very fine droplets could be achieved (<200 micrometers) and air flow rates of above 130 m³/h would be applied. If air is heated to 50 °C, droplet diameters of up to 400 micrometers could be evaporated within 10 seconds - also with relatively high specific air flow rates. An air temperature of 60 °C would be feasible with almost the entire investigated parametric field. Raising the temperature to 70 °C would reduce the required evaporation time by almost 50% on average.

Practically, it can be expected that the lower the required air temperature is, the higher the applicability of spray evaporation. Utilization of waste/ excess heat from industrial processes or use of inexpensive solar collectors would enhance the feasibility of zero-liquid discharge by spray evaporation. Thus, as a general requirement it was concluded that experimental tests with a minimum temperature of 50 °C should be conducted. Since this parametric study is based on assumed conditions it is crucial to test the droplet evaporation in practice. By performing experimental test series with variation of air flow rates, temperatures and spraying rates the model could be also validated/ corrected and used to design a prototype evaporation unit in the next development step of NoBriner's brine treatment solution.



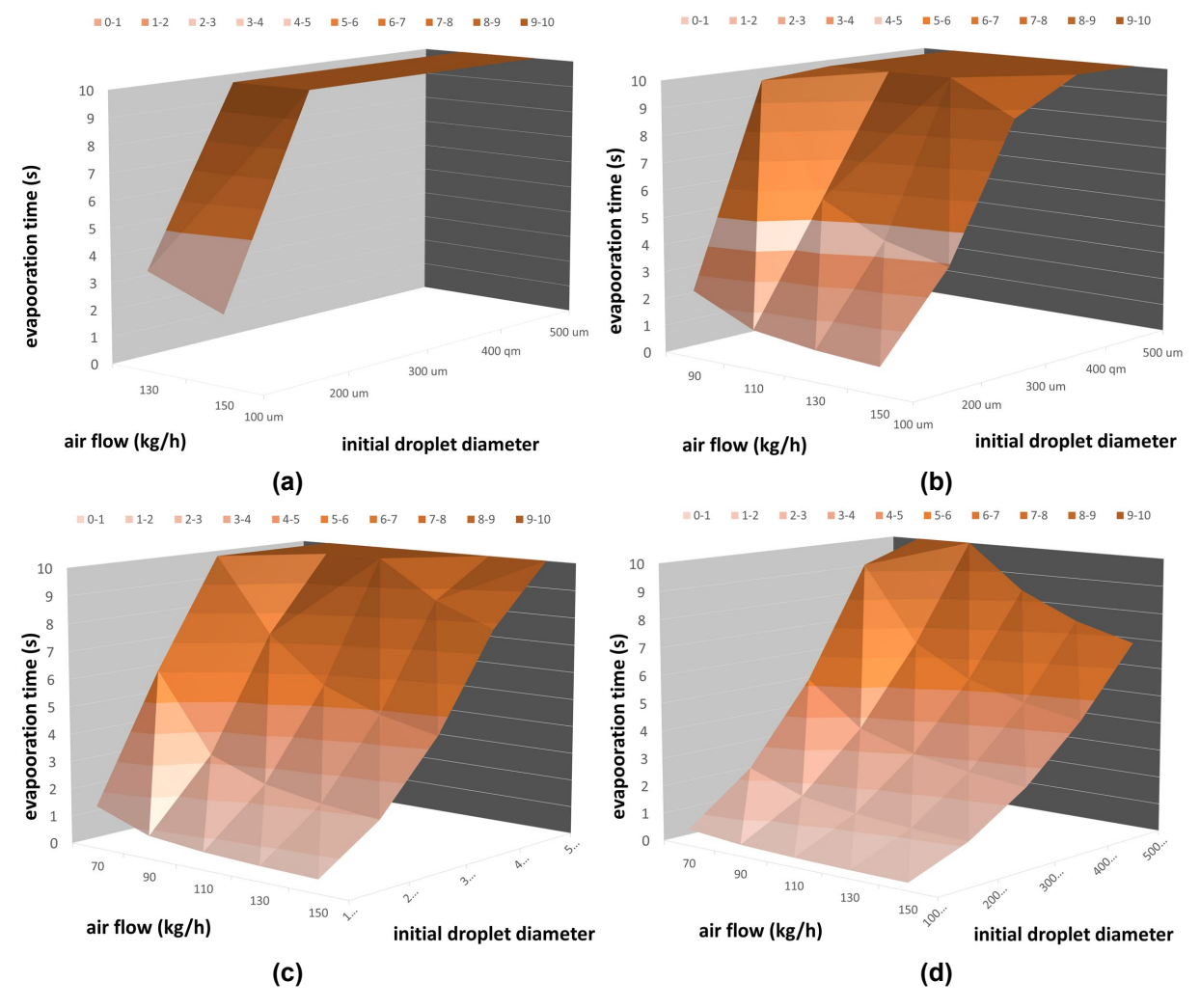


Fig. 4.13: Sensitivity analysis of droplet evaporation with initial droplet diameters ranging from 100-500 micrometers, a initial droplet temperature of 30 °C, inlet air humidity of 6.5 g_water/kg_dry air and a spraying rate of 1 kg/h - employing the following variations of inlet air conditions:

- a) Temperature=40 °C; r.h.=14.2%;
- b) Temperature=50 °C; r.h.=8.5%
- c) Temperature=60 °C; r.h.=5.3%;
- c)Temperature=70 °C; r.h.=3.4%

TRNSYS water droplet evaporation model (type 1020)

A new TRNSYS component Type 1020 is developed based on the water spray evaporation model. The difference is that Type 1020 will further calculate the total number of water droplets according to the water flow rate and the time step defined by users. All droplets are assumed to be heated by surrounded hot air in the same condition and do not interact with each other. The output will sum up all the water vapor mass and the left droplets to output the evaporation and the discharge water mass. The parameters, inputs and outputs can be set in Type 1020 are listed in Table 4.2.



Users should provide a precise simulation time step according to the spray evaporation device. The simulation time step is the maximum residence time of a water droplet in the spray evaporation device, which depends on the device dimension and the water flow rate.

Type 1020 can only calculate one droplet diameter case but more Type 1020 components can be dragged into TRNSYS projects in order to simulate more droplet diameters.

The limitation of Type 1020 is that it only simulates the evaporation process of pure water droplet, which will typically take more time of evaporation than brine droplet and in this way, it will output more conservative results compared to the brine droplet case.

In order to simulate the evaporation limit of a brine droplet, the parameter EvapRatioThres is defined. The usage of this parameter is described in the comments of Table 4.2.

A TRNSYS system example using Type 1020 is developed and introduced in section 6.

Table 4.2. Parameters, Inputs and Outputs of Type 1020

| Parameters | Unit | Comments |
|------------|----------|--|
| hw | kJ/kg | The latent heat of evaporation of water |
| Mw | kg/kmol | The molar mass of water |
| Ма | kg/kmol | The molar mass of dry air |
| р0 | Ра | The ambient pressure |
| Ru | J/kmol·K | The universal gas constant |
| alpha | - | The thermal accommodation coefficient |
| alpham | - | The mass accommodation coefficient |
| lambdas | m | The mean free path of the surrounding air |
| Zair | - | Compressibility factor for air at 1 atm |
| Срw | kJ/kg·K | Specific heat capacity of water at 293.15 K |
| Cpwv | kJ/kg·K | Specific heat capacity of water vapor at 300 K |
| sigmaw | N/m | Surface tension of water |
| BoundCon | - | Boundary condition. 0 for adiabatic condition and other value for isothermal condition |



| EvapRatioThres | % | The threshold of evaporation to simulate brine solution. In this model, calculations can only be carried out from the original brine solution to the start of salt separation, where there is a salt maximum percentage, fx 25%. Therefore, EvapRatioThres = 100- 1/0.25*saltpercentage. For salt percentage is 7% of brine solution. EvapRatioThres is 72% |
|----------------|------------|---|
| Inputs | Unit | Comments |
| DropDia | m | Droplet diameter 1 |
| DropTemp | °C | Droplet Inlet temperature |
| WaterFlow | Liter/hour | Volume flow rate of inlet water |
| AirTemp | °C | Air Inlet temperature |
| RelHumd | RH | Initial relative humidity of surrounding air |
| AirFlow | kg/h | Mass flow rate of inlet air |
| Outputs | Unit | Comments |
| DropDiaOut | m | Outlet droplet diameter |
| DropTempOut | °C | Outlet droplet temperature |
| RelHumdOut | RH | Outlet relative humidity |
| AirTempOut | °C | Outlet air temperature |
| MassInitial | kg | Initial water mass |
| MassEvaporated | kg | Evaporated water mass |
| EvapRatio | % | Evaporation ratio |
| VaporFlowrate | kg/hr | Water vapor flowrate |
| Ndroplet | - | Number of Droplets |
| MassLeft | kg | Unevaporated Mass |



5. Preparation of experimental investigations

It was decided to prepare for building an experimental setup to elucidate the limit of evaporated spray evaporation and to determine the right components (e.g. choice of spraying nozzles). Consequently, the droplet evaporation model (pure water) was used as basis for component sizings. By running experimental tests with simulated conditions it would be possible to validate/correct the droplet simulation model. The validated model could be thereafter used for planning of full-size spay evaporation units - as key component of the NoBriner brine treatment solution.

Test setup

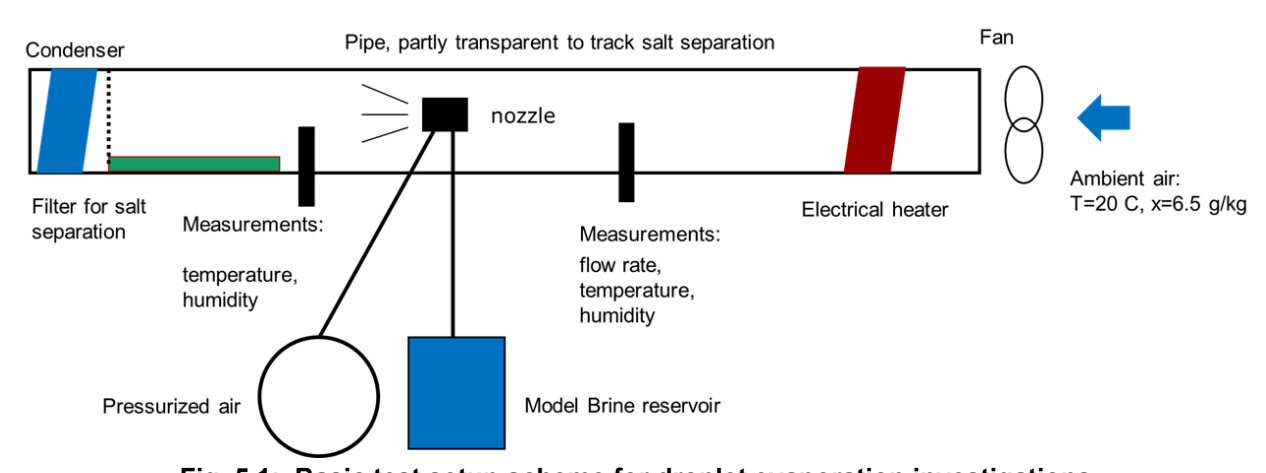


Fig. 5.1: Basic test setup scheme for droplet evaporation investigations

To experimentally investigate droplet evaporation under various ambient conditions a test setup utilizing ambient air was designed. A scheme is presented in Fig. 5.1 - the main components and their designed functionalities are the following:

- **Pipe:** The pipe is designed in order to realize optimal flow conditions (diameter, length). The section after the nozzle is transparent in order to visually track salt separation during droplet evaporation.
- Fan: A fan, located at the inlet of the test setup, blows ambient air into the pipe. It can be varied in speed in order to regulate air flow rates to optimize droplet evaporation in dependency of spray rate and ambient air conditions.
- **Electrical heater:** Heating power is adjusted in order to raise the temperature of the ambient air sufficiently to enable full evaporation of sprayed brine.
- Measurement equipment: To measure air flow rates an anemometer is installed at the
 after the electrical heater. Combined humidity and temperature sensors before and after
 (sufficient distance to nozzle) brine spraying nozzle are used to monitor the change of air
 states during the droplet evaporation. Measurements are obtained via a data logger.
- Nozzle and pressurized air supply: Two-component nozzles (utilizing pressurized air for brine spraying) were chosen - see component sizing. A compressor is supplying air set pressure and suction heat to the brine reservoir determine the brine spraying rate.



- Model brine reservoir: As described in section 2, NaCl is the dominating salt in typical brine sources. Since no significant effect is expected, the model brine is prepared as a mixture of filtered water and NaCl.
- Filter for salt separation: To demonstrate the feasibility of zero-liquid discharge of brine by spray evaporation salt particles are separated by the air flow by means of a filter - particle filter from HVAC installations.
- **Condenser:** To demonstrate regain of pure water, a cooled coil (realized by circulation of cold water) is installed at the end of the test setup. The water is separated by condensation on the coil surface and can be collected via a bucket below the condenser (at the end of the pipework)

Component sizing

Assuming low heat losses of the pipework (e.g. by insulation of parts of the pipework and relatively high air flow rates), an adiabatic evaporation process (constant air enthalpy) can be assumed resulting in cooling of the air while raising its water content. To enable full evaporation of sprayed brine, ambient air must be preheated. An example calculation assuming a spraying rate of 1 kg brine/ hour and an air flow of 100 kg/h (relatively high value in order to lower pre-heating requirements) was conducted - results are visually shown in the Mollier-Diagram below (Fig. 5.2), calculation steps can be found in Table 5.1.

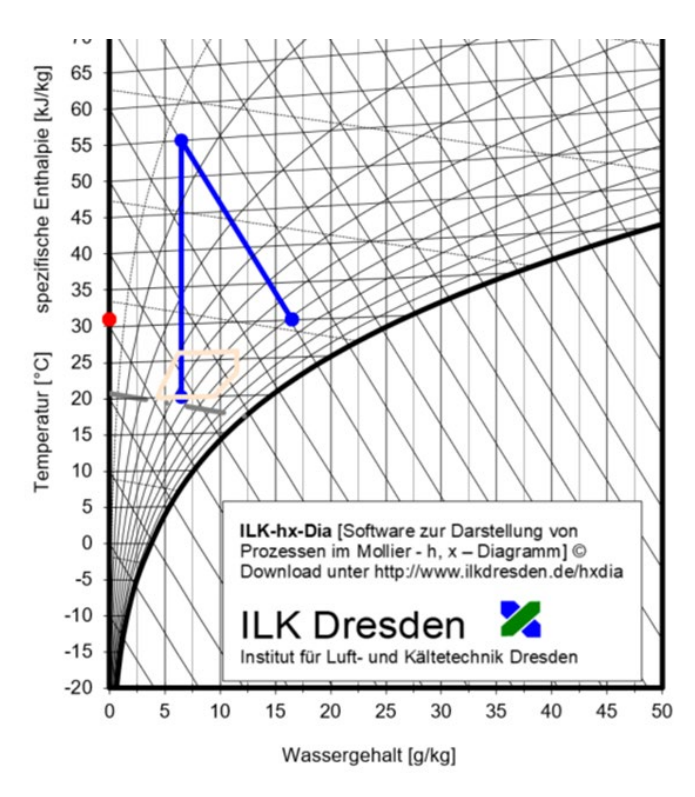


Fig. 5.2: Two states of the spray evaporation process - first pre-heating from ambient conditions to 55 °C, then adiabatic evaporation.



| Luftdruck [Pa] | 101 | ,325 | Der Normalluftdruck beträgt 101 325 Pa, oft wird vereinfacht 1 bar (100 000 Pa) verwendet. | | | | | | Masse- strom | 100 | kg/h | | |
|--------------------------------|------------|-----------|---|--------------|------------|--------------|------------------|-------------------------|----------------------------|-----------|--------|-------------------|----------------------|
| Bezeichnung | Temperatur | Enthalpie | rel. Luftfeuchte | Wassergehalt | Temperatur | Wassergehalt | rel. Luftfeuchte | Taupunkt- temperatur | Feuchtkugel- temperatur | Enthalpie | Dichte | Volumen- strom | wirksame Leistung |
| | °C | kJ/kg | % | g/kg | °C | g/kg | % | °C | °C | kJ/kg | kg/m³ | m³/h | kW |
| Ambient condition | 20.0 | | | 6.50 | 20.0 | 6.5 | 44.8 | 7.7 | 13.0 | 36.7 | 1.20 | 83 | |
| Required heating power: 1000 W | | | | 6.5 | 55.0 | 6.5 | 6.7 | 7.7 | 24.0 | 72.5 | 1.07 | 93 | 1.0 |
| Spray evaporation 1 kg/h | 30.0 | | | 16.5 | 30.0 | 16.5 | 61.7 | 21.8 | 24.0 | 72.5 | 1.15 | 87 | 0.0 |

Table 5.1: Calculation steps corresponding to Fig. 5.2.

 \rightarrow With the chosen conditions, the process can be theoretically run with a specific heating power of 1000 W - leaving a safety margin to the associated dew point (about 24 °C).

Based on this fist assessment, the droplet evaporation model (pure water as most conservative variant) was applied. To gain crystallized salt, a brine concentration of approximately 50% or higher is needed [3]. Thus is was decided to calculate with an evaporation end criterion of 90% mass evaporation - this corresponds to a final brine concentration of 70% when using brine from seawater desalination (section 1). Results on droplet evaporation are shown in Fig. 5.3. A standard droplet diameter distribution of 20-500 micrometers with 2-component nozzles in stainless steel (see choice of nozzle) was assumed. To keep evaporation time below 10 seconds, an inlet air temperature of 60 °C was chosen - consequently air flow rates should be above 100 kg/h to ensure sufficiently high evaporation rates.

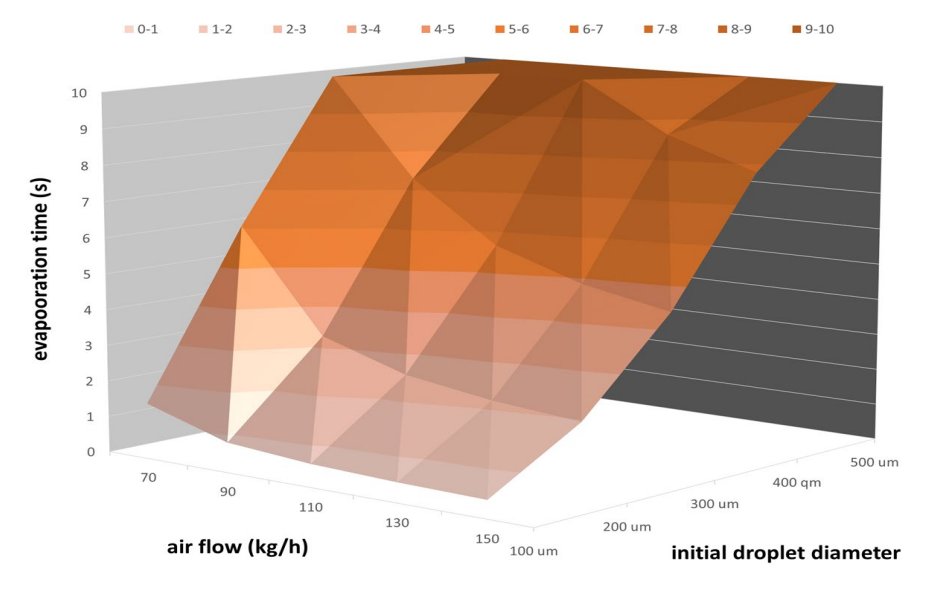


Fig. 5.3: Droplet evaporation time study considering the following parameters: Inlet air temperature = 60 °C, inlet air humidity = 6.5 g/kg, brine temperature = 30 °C, spraying rate = 1 kg/h.

Regarding the choice of the right spraying setup, MT Spray AS (sales engineer Claus Brandt) was consulted. When discussing the possibility to utilize standard nozzles for hydraulic injection spraying it was quite clear that this is not the optimal choice (however, potentially the cheapest) because high pressure (above 7 bar - at least) would be needed to achieve fine droplets. Thus,



to achieve a fine droplets with a nozzle appropriate for the applied air temperature (max. 70 °C), and to minimize the risk for clogging of the nozzle, the following two options have been defined (illustration in Fig. 5.4):

- Siphon-fed spray setup utilizing air atomizing nozzle: The spraying rate can be adjusted by air pressure and suction head.
- Pressure spray setup utilizing air atomizing nozzle: Both brine and air are pressurized pressure change for adjustment of the spraying rate.

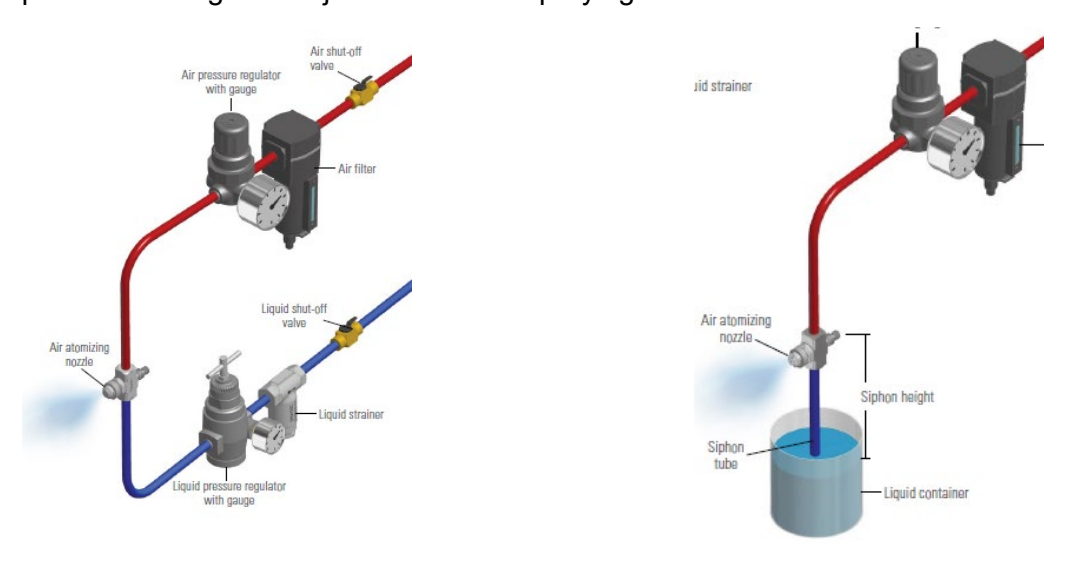


Fig. 5.4: Pressure spray setup (left), Siphon-fed spray setup (right) [20].

Fine droplets are achieved due to mixing at the nozzle outlet [20]. According to Claus Brandt, polymeric nozzles typically generate droplets with diameters in the range of 100 to 1000 micrometer - while nozzles in stainless steel generate droplets with a diameter range of 20-500 micrometer. With the siphon-fed spray setup the amount of needed components is reduced - also in comparison to hydraulic injection, where a pump must maintain high brine pressure (difficult to achieve with low spraying rates).

Consequently, spray equipment in stainless steel for a siphon-fed setup was chosen:

Air atomizing nozzle incl. Fluid cap, air cap and supporting structure - setup no. SU1 Costs according to offer from 16.04.2020: 8.171,90 DKK excl. moms.

With this setup spraying rates from 0.8 - 3.7 l/h can be realised. The full properties incl spray ange can be found in Table 5.2:



Table 5.2: Properties of the chosen spray setup with air atomizing nozzle (catalogue[20] - section D3)

| Spray Set-up No. | Spray Set-up Consists of Fluid and Air Cap Combination | Atomizing Air | | Liquid Capacity (liters per hour)* | | | | | | | | Spr at 20 c |
|------------------------|---|------------------|-------------------|---------------------------------------|-----|-----|--------------|-----|-------|-----|-----|----------------|
| | | Air | ir All | | | | non Height (| | Spray | | | |
| | | Press. | Capacity I/min | 45 | 30 | 15 | 10 | 20 | 30 | 60 | 90 | Angle A (°) |
| | Fluid Cap 2050 + Air Cap 64 | .70 | 13.3 | 2.4 | 2.1 | 1.7 | 1.5 | 1.2 | .79 | _ | _ | |
| 0114 | | 1.5 | 20 | 2.8 | 2.6 | 2.4 | 2.1 | 1.9 | 1.6 | .91 | _ | 18 - 19 |
| SU1 | | 3.0 | 32 | 3.4 | 3.1 | 2.9 | 2.8 | 2.6 | 2.4 | 1.7 | 1.1 | |
| | | 4.0 | 41 | 3.7 | 3.4 | 3.3 | 3.1 | 2.9 | 2.7 | 2.1 | 1.5 | |

Range of air flow rates: The air flow rate must be adjusted in dependency of the actual spraying rate - approximately in the range of 100-200 m³/h

Range of heating power: Consequently, heating power must be adjustable from 1000 to 2000 W.

Pipe diameter: Pipe diameter must be chosen in order to match the needed air flow rate, as well as spraying angle at the nozzle. For flow rate of 100 m³/h and a pipe diameter of 400mm the air velocity is 0.22 m/s. Assuming a droplet evaporation time of 10 seconds, the pipe must be 2.2 m long. Furthermore, to ensure accurate measurements of air properties, a pipelength of 2 diameters before and 3 diameters after measurements points must be realized without change of air properties or pipe diameter.

Brine reservoir: A wide brine reservoir, containing about 50 litres seems appropriate to maintain syphon heads almost constant during several hours of operation.

Selected equipment and fist preparations at DTU Byg

DTU Byg has a stock of used equipment from previous projects at its prototype test facility. Thus, it was offered to NoBriner to merely create a test setup by re-use of used components, which have been selected as follows:

To enable measurements up to 6 m from the data logging cards combined humidity and temperature sensors and an anemometer with extended cables could be utilized from an existing experimental setup (Fig. 5.5, left). The equipment is already connected to an agilent data logging equipment (Fig. 5.5, right) - measurements can be monitored and stored via pre-installed PC applications.







Fig. 5.5: Two combined humidity and temperature sensors and one anemometer for air property measurements (left); Agilent data logging equipment with analogue data logging cards (right).

A rig with a variable-speed fan (nominal max. air flow rate of 200 m³/h), a variable power (max. 2000W) heating register and a flow reduction valve for manual optimization of air flow rates was pre-assembled (Fig. 5.6). It was planned to extend the rig with an transparent plexiglas-pipe with a diameter of 400 mm (leght = 1250 mm) via three junctions - as applied in another project (Fig. 5.7, left). The nozzle could be placed before this plexiglas pipe. Additionally 3 m of plexiglas pipes with reduced diameter (Fig. 5.7, right) would be available to track the droplet evaporation process visually.



Fig. 5.6: Pre-assembled air conditioning rig - manual air flow control valve (right), adjustable fan with (middle), heating register with variable power (left).





Fig. 5.7: Example for integration of an transparent Plexiglas-pipe with three junctions - currently used in another project (left); two plexiglas pipes with flanges on stock - 1500 x 240 mm, (right).



A membrane expansion vessel (Fig. 5.8) could be utilized as brine reservoir with a brine capacity of about 50 I. It could be utilized pressure-less for siphon-fed spray setup as well as in a pressured spray setup in order to test alternative nozzles without pressurized air - in this case a pre-pressure of max. 5 bar could be applied to the membrane vessel.



Fig. 5.8: Membrane expansion vessel, possible use as brine reservoir.

The test setup could not be finalized due to financial limitations (purchase of additional pipework material, spray nozzles, fittings, etc. would be needed). The goal is to continue the collaboration and to perform experimental tests with NoBriner at a later point.



6. System aspects

Utilization of a spray evaporation unit requires additional components such as a condenser to harvest both, solidified salt (hypersaline) and pure water. In this section assessments are presented to elucidate possibilities/ limitations of a stand-alone desalination solution, utilising spray evaporation - with the ultimate goal of zero-liquid discharge.

Assessment tool: solar electricity production

Considering that the spray evaporation system can not be a standalone solution due to its high energy consumption, the possible usage of PV panels for the production of the energy required by the ZLD system was analysed through Python, thanks to the open-source library PVLib.

PVLib is a library which was firstly created for Matlab and then ported to Python, and it has already been used for several scientific publications. It was originally created by the Sandia National Laboratories for the United States Department of Energy's National Nuclear Security Administration, and it was ported to Python in 2014. [21]

Since the price of PV Panels drops constantly, and the NoBriner target are arid regions with low technical expertise, it was thought that PV solar panels which just require mounting and wiring could serve as a good way to provide the electricity needed by the desalination system.

It was therefore created a python script which simulates the electrical energy production from PV Solar Panels, depending on several user-specified parameters:

- Energy Need (W)
- Location (Name of the place)
- Surface Tilt of the panel (°)
- Surface Azimuth of the panel (°)

The weather information is taken from the PVGis portal (EU Science Hub, an official EU Website) [22] through the Typical Meteorological Year (TMY) tool. Even though PVGis includes also a PV Performance Tool, the data was output on a monthly basis, while for a correct assessment of the energy provided by the solar system a hourly output was preferred, which is something possible with the PVLib.

As an example, the city of Kakuma in Kenya was used for the simulation.

Thanks to the TMY, it was possible to gather Temperature, Wind Speed and Irradiance data from the closest weather station to Kakuma for every hour of the year, as can be seen from Table 6.1.



Table 6.1: Data output from the PVGis TMY

| | time_corr_UTC | temp_air | wind_speed | ghi | dni | dhi |
|------|----------------|----------|------------|-----|-----|-----|
| 0 | 01-01 00:00:00 | 25.94 | 1.66 | 0.0 | 0.0 | 0.0 |
| 1 | 01-01 01:00:00 | 25.65 | 1.67 | 0.0 | 0.0 | 0.0 |
| 2 | 01-01 02:00:00 | 25.37 | 1.68 | 0.0 | 0.0 | 0.0 |
| 3 | 01-01 03:00:00 | 25.08 | 1.69 | 0.0 | 0.0 | 0.0 |
| 4 | 01-01 04:00:00 | 24.79 | 1.70 | 6.0 | 0.0 | 6.0 |
| | | | | | | |
| 8756 | 12-30 20:00:00 | 30.87 | 2.00 | 0.0 | 0.0 | 0.0 |
| 8757 | 12-30 21:00:00 | 30.35 | 2.15 | 0.0 | 0.0 | 0.0 |
| 8758 | 12-30 22:00:00 | 29.83 | 2.30 | 0.0 | 0.0 | 0.0 |
| 8759 | 12-30 23:00:00 | 29.30 | 2.46 | 0.0 | 0.0 | 0.0 |
| 8760 | 12-31 00:00:00 | 28.44 | 2.74 | 0.0 | 0.0 | 0.0 |

The intermediates needed for the calculation of the power output were calculated from this data through PVLib. These were Extraterrestrial Radiation, Airmass, Diffuse Sky Radiation (Hay Davies model), Ground Diffuse Radiation, Angle of Incidence, Total Irradiance and Cell Temperature.

It will be presented in Fig. 6.1 the Plane of Array radiation as an example of those calculations.

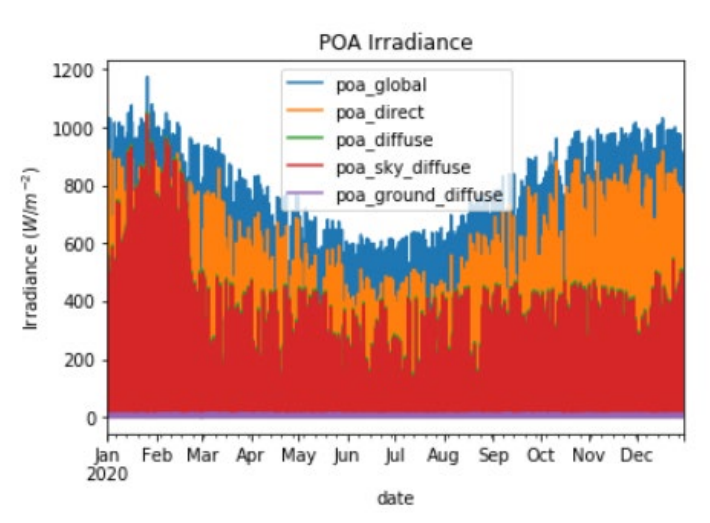


Fig. 6.1: Plane of Array radiation throughout the year

Depending on the user needs, two different solar kits were taken into consideration. For a consumption of 3.6 kW or more, a 6 kW PV kit was considered, while for a consumption of less than 3.6 kW, a 3.6 kW PV kit was considered. Both kits are from Grape Solar, and they are sold on the website Home Depot. [23] [24]



Kits were chosen because they include an inverter, which would make the installation easier. Specifications of panels allowed to predict the DC output of the solar kit on a hourly basis through the PVWatts model, provided by the National Renewable Energy Laboratory (NREL) [25]:

$$P_{mp} = \frac{E_e}{E_0} P_{mp0} \left[1 + \gamma \left(T_c - T_0 \right) \right]$$

P_{mp}: Maximum Power Point (W)

E_e: Effective Irradiance (W*m⁻²)

E₀: Reference Irradiance (1000 W*m⁻²)

P_{mp0}: Nominal Power (W)

y: Temperature Coefficient (°C-1)

T_c: Cell Temperature (°C)

T₀: Reference Temperature (25 °C)

Both the inverters included in the kits were present on the Sandia Laboratories Database, which allowed to convert the AC output to a DC output, including also the inverter consumption. This conversion was made through the Sandia Inverter Model [26]:

$$\begin{split} P_{AC} &= \left\{ \frac{P_{AC0}}{A-B} - C\left(A-B\right) \right\} \left(P_{DC} - B\right) + C\left(P_{DC} - B\right)^2 \\ &\text{with:} \\ A &= P_{DC0} \left\{ 1 + C_1 \left(V_{DC} - V_{DC0}\right) \right\}, \\ B &= P_{s0} \left\{ 1 + C_2 \left(V_{DC} - V_{DC0}\right) \right\} \text{ and} \\ C &= C_0 \left\{ 1 + C_3 \left(V_{DC} - V_{DC0}\right) \right\}. \end{split}$$

V_{DC}: DC Input Voltage (V)

 V_{DC0} : DC Voltage Level at which the AC power rating is achieved at ref. operating conditions (V)

P_{AC}: AC Output Power (W)

P_{AC0}: Maximum AC Power Rating for inverter at reference conditions (W)

P_{DC0}: DC Power Level at which AC power rating is achieved at reference operating conditions (W)

P_{s0}: DC Power required to start the inversion process (W)

C₀: Parameter defining the curvature of the relationship between AC output and DC input power

C₁, C₂, C₃: Empirical Coefficients (V⁻¹)

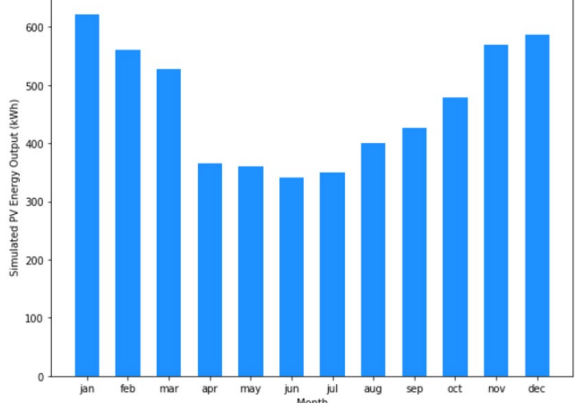


In order to ensure that the output values were valid, a validation on a monthly basis was carried out, comparing the results from the model and the data retrieved from PVGis (Table 6.2).

Table 6.2: Comparison of monthly energy yield for validation

| Month | PVLib output (kWh) | PVGis output (kWh) | Error (%) |
|-----------|--------------------|--------------------|-----------|
| January | 621 | 638 | 2.56 |
| February | 560 | 537 | 4.31 |
| March | 528 | 507 | 4.06 |
| April | 366 | 400 | 8.60 |
| Мау | 361 | 372 | 3.07 |
| June | 342 | 335 | 1.93 |
| July | 351 | 357 | 1.64 |
| August | 401 | 415 | 3.30 |
| September | 427 | 476 | 10.39 |
| October | 479 | 521 | 8.07 |
| November | 570 | 531 | 7.21 |
| December | 587 | 611 | 3.84 |
| TOTAL | 5591 | 5699 | 1.89 |







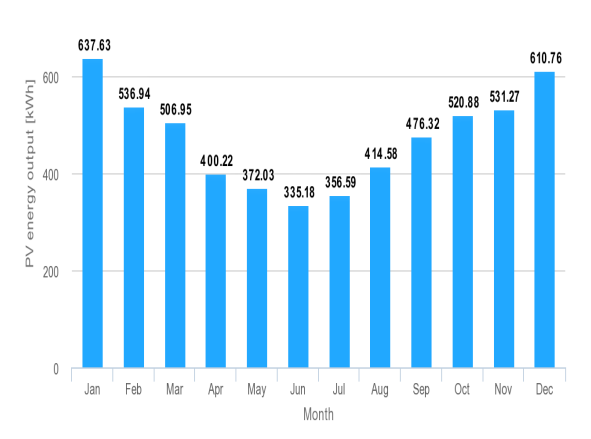


Fig. 6.3: PVGis Energy Output per Month (kWh DC)

As can be seen from the Table above and from the Figures 6.2 and 6.3, while in 4 months over 12 the error overcame 5%, in 8 months over 12 the error was inferior to 5%. The model is therefore generally valid, but more analysis will be done to understand the discrepancy in the 4 months with error bigger than 5%. Moreover, the error throughout the year is below 2%.

The creation of a solar resource assessment tool is a part of a broader future tool which will enable NoBriner to communicate to the final customer the cost of installing a ZLD solution, not only from the perspective of the device itself, but also from an energetic point of view. The relevance of PV for a ZLD system depends on the area where this system would be set up, since it depends by the availabilty of natural energy resources (wind, sun, hydropower..).

PV has an undoubted potential to provide low-cost energy to rural areas, and this potential could be better understood with a study on the mounting, shipping and maintaining costs of the PV system.

More studies will be carried out to make the system standalone with no need of grid connection, also including wind energy and heat pumps.



Numerical investigation on system integration of a spray evaporation unit

A system using the spray evaporation unit is designed as shown in Figure 6.4.

The system contains a spray evaporation unit, a solar air collector, a fan, a condenser and a pump for providing the brine. The spray evaporation unit contains three spray nozzles. Solar air collector is used to heat the ambient airflow and the outlet airflow is blown into the evaporation unit. The brine will be pumped and sprayed into the evaporation unit as small droplets by the nozzles. The small brine droplets in the unit will be heated by the hot airflow and some of the water will be evaporated into the water vapor. Then the water vapor is guided into the condenser and condensed into pure water. The discharged high concentration salt brine in the unit will be collected. The cold brine is pumped in the condenser for preheating.

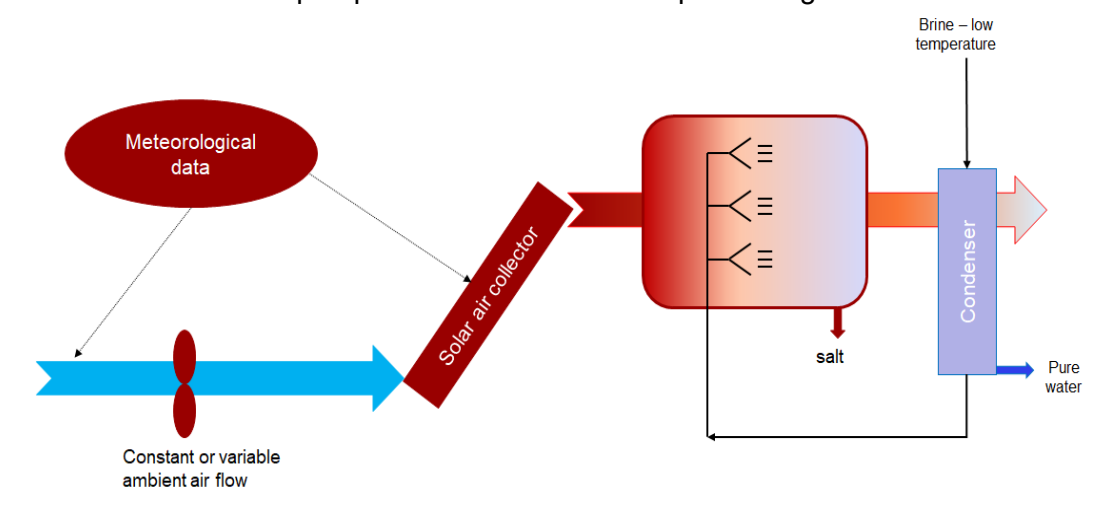


Fig. 6.4: System diagram

According to the system design, a TRNSYS project was created as shown in Fig. 6.5. Three Type 1020 (described in section 4) were used for simulating the spray evaporation process with the droplet diameters that provided by users. A weather component was used to provide the weather data of Nairobi, Kenya. A controller was designed for controlling the start and stop of the fan and pump. The controller gave positive signals when the solar radiation was larger than a presetting value, for example 100 W/m². A solar air collector was used and the collector area and the slope can be set by users. The flow diverter diverts the outlet airflow into the three spray evaporation nozzles. Three condensers are created corresponding to the three nozzles. All the discharged salt and condensed water are summed up from the three spray evaporation devices and from the condensers. An integration type was used to sum up the discharged salt, condensed water and the electricity consumption of the Fan and the Pump. The hourly results were red by Type 25c and written into an output file.



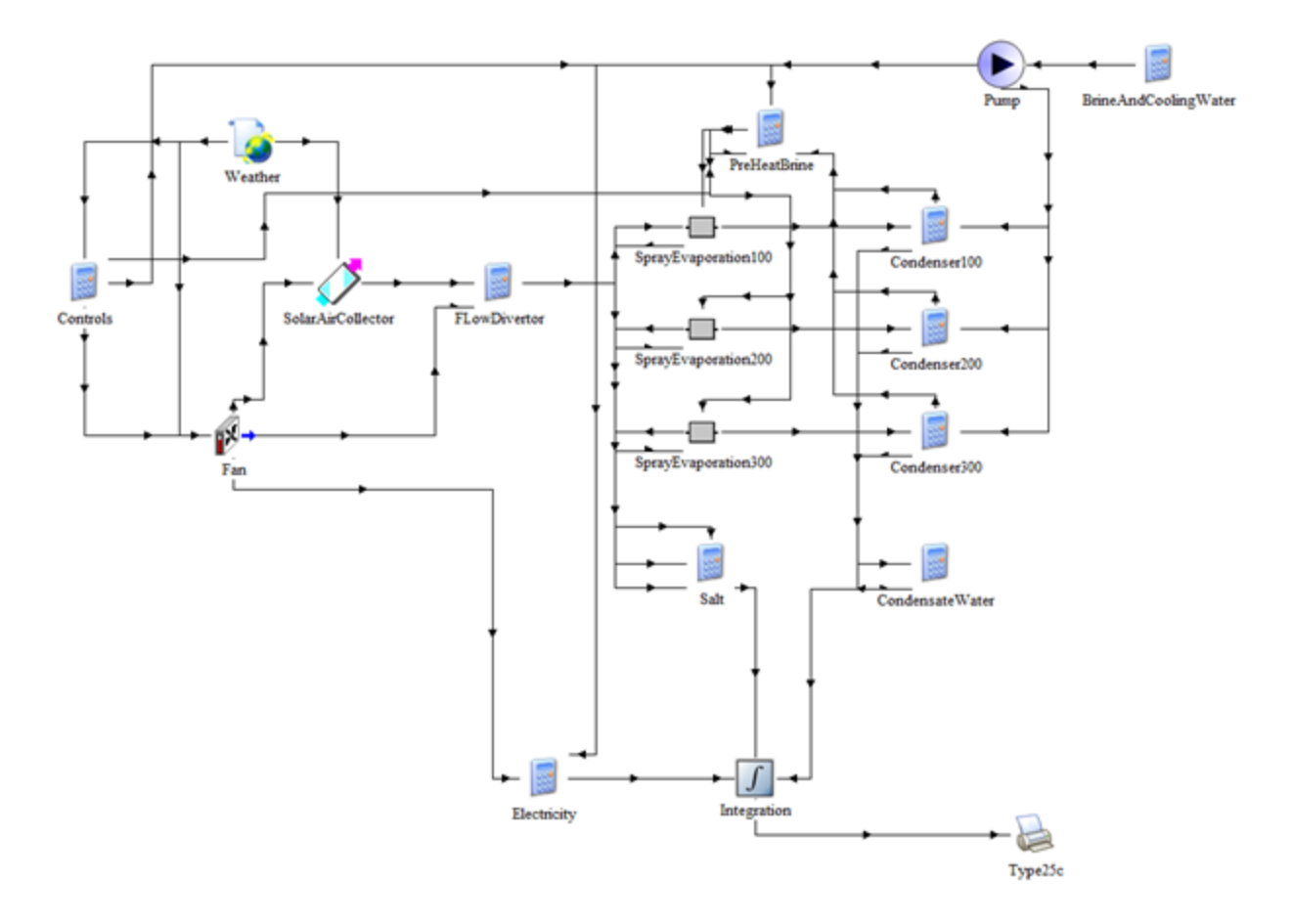


Fig. 6.5: System simulation in TRNSYS studio platform

The developed system in TRNSYS studio platform is a simplified and ideal version. The following limitations needs to be considered when using the system simulation:

- 1) Pure water droplet is used in the spray evaporation unit. However, the spray evaporation unit Type 1020 can limit the water mass evaporation ratio in order to simulate the brine droplet evaporation.
- 2) Condenser is designed as an ideal heat exchanger for simplicity. The condensation temperature is assumed at 1° degree below the dew point temperature. The condensate sensible heat and latent heat can be fully transferred to the cooling fluid and the outlet temperature of the cooling fluid will reach the condensation temperature.
- 3) The brine flow rate for preheating is only 1-2 liter/hour, which is far too low for condensing the water vapor. Therefore, a total of 10, 20 and 30 liter/hour cooling water flow rate is used for condensation purposes.

An example of the system simulation was created. The aim of the system simulation was to carry out parametric studies of the system aiming to approach 90% evaporation rate.



The constant parameters are listed here. The initial salt concentration of the brine was 7%. The weather data file was TMY Nairobi, Kenya. The solar air collectors have a 6 m² area with a slope of 0°. The fan was set with a constant airflow at 150 kg/h and the airflow diverter distributed 50 kg/h of airflow for each spray evaporation nozzle. Each nozzle had an inlet water flowrate of 1 l/h.

The time step, the droplet diameter of each nozzle and the horizontal solar radiation threshold for activating the fan and the pump were the variables. The cooling fluid was not added for showing the limitation. The unevaporated water and the condensed water were collected and summed up for the whole year simulation period and output into a file. The evaporation rate of each case was calculated. The power consumption of the fan and pump were calculated according to the standard settings of the TRNSYS.

The results of the total 8 scenarios are summarized in Table 6.3. It can be seen from the table that the longer time step, the smaller droplet diameter and the higher solar radiation threshold lead to higher evaporation ratio. The evaporation ratio in the 8 scenarios varied from 71% to 85.1%.

Table 6.3: Results summary for a whole year simulation using 50 kg/h airflow.

| Scen ario | Tim e step | Solar radiation threshold | Droplet diameter of each nozzle | Operat ion time | Water inlet | Unevapora ted water | Conde nsed water | Uncondens ed water vapor | Evapor ation rate |
|--------------|------------------|---------------------------------|---------------------------------------|-----------------------|----------------|------------------------|------------------------|--------------------------------|-------------------------|
| Unit | s | W/m² | um | h/y | I/y | l/y | I/y | I/y | % |
| 1. | 25 | 500 | 100/200/300 | 1673 | 5018 | 1457 | 87 | 3474 | 71 |
| 2. | 30 | 500 | 100/200/300 | 1673 | 5018 | 1354 | 80 | 3584 | 73 |
| 3. | 20 | 500 | 100/100/100 | 1673 | 5018 | 942 | 86 | 3990 | 81.2 |
| 4. | 25 | 500 | 100/100/100 | 1673 | 5018 | 920 | 87 | 4011 | 81.7 |
| 5. | 25 | 600 | 100/200/300 | 1280 | 3837 | 966 | 70 | 2801 | 74.8 |
| 6. | 30 | 600 | 100/200/300 | 1280 | 3837 | 888 | 69 | 2880 | 76.9 |
| 7. | 20 | 600 | 100/100/100 | 1280 | 3837 | 586 | 73 | 3178 | 84.7 |
| 8. | 25 | 600 | 100/100/100 | 1280 | 3837 | 570 | 73 | 3194 | 85.1 |



The additional 4 scenarios were investigated for higher airflow of 125 kg/h of each nozzle - results are presented in Table 6.4. The solar collector area was increased to 8 m^2 in the last two scenarios. The time step, solar radiation threshold and droplet diameter of each nozzle were varied. It can be seen from the table that by using the high airflow with a shorter time step (10s) and low solar radiation threshold (500 W/m²), the resulting evaporation rate was lower than 50%. However, by increasing the time step, the solar air collector area and the solar radiation threshold, the evaporation rate was increased up to 74.1%. When the droplet diameters of the three nozzles were decreased to the average 100 um, the evaporation rate exceeded 90%.

Table 6.4: Results summary for a whole year simulation using 125 kg/h airflow.

| Scenari o | Time step | Solar air collect or area | Solar radiatio n thresh old | Droplet diameter of each nozzle | Operati on time | Water inlet | Uneva porate d water | Conde nsed water | Uncon densed water vapor | Evapora tion rate |
|--------------|--------------|------------------------------------|---|---------------------------------------|--------------------|----------------|-------------------------------|------------------------|-----------------------------------|----------------------|
| Unit | s | m² | W/m² | um | h/y | I/y | I/y | I/y | I/y | % |
| 1. | 10 | 6 | 500 | 100/200/300 | 1673 | 5018 | 2595 | 81 | 2342 | 48.3 |
| 2. | 20 | 6 | 700 | 100/200/300 | 924 | 2772 | 863 | 51 | 1858 | 68.9 |
| 3. | 25 | 8 | 600 | 100/200/300 | 1280 | 3837 | 994 | 76 | 2767 | 74.1 |
| 4. | 25 | 8 | 600 | 100/100/100 | 1280 | 3837 | 281 | 73 | 3483 | 92.7 |

In conclusion, the functionality of the droplet evaporation model was demonstrated with a simplified system model in TRNSYS environment. Users can change the power settings and the type of heat source (e.g. collector type) according to local circumstances. More spray evaporation units could be used in applications in order to produce more unevaporated water and condensed water. By adding the cooling flow rate (assuming an additional cold water source) it would be possible to condense more water after the evaporation process. Since the brine inlet flow was considered as the only cooling flow with a low flowrate 1 l/h, most of the water vapor is not condensed and discharged to ambient air.



7. Conclusions

NoBriner aims for a stand-alone solution to manage brine by zero-liquid discharge spray evaporation. Regarding future technology development, the work output should be considered as follows:

- Literature: Most relevant definitions and a technology overview of spray evaporation processes for desalination were identified. Stand-alone spray evaporation systems were reported for systems utilizing solar collectors as heat sources.
- Brine characteristics: Ideally, a spray evaporation unit will have to cope with brine concentrations ranging from dilute 0.3% to highly saline 7%. Future simulation and experimental setups should investigate the impact on evaporation kinetics of complex brine compositions.
- Based on previous work described in literature, a validated pure water droplet spray evaporation model was further developed and implemented in Python programming environment. The model can simulate the evaporation process of a pure water droplet heated by warm air around in the horizontal tube. Furthermore, a brine droplet spray evaporation model was developed, which simulates a brine droplet evaporation process with the real time updated brine properties.
- To implement a spray evaporation unit in system simulation, a TRNSYS type was developed based on the Python model on pure water droplet evaporation.
- An experimental spray evaporation setup was planned incl. choice and sizing of components. This setup should be used to prove the functionality of zero-liquid discharge and to validate/correct the developed droplet spray evaporation models.
- The functionality of the droplet evaporation model (pure water) was demonstrated with a simplified system model in TRNSYS environment. Simulation of a whole year's water spray evaporation process is achieved with the limitation of ideal conditions and presumptions. However, to be able to evaluate the application potential of a stand-alone spray evaporation solution, the following work steps are still required:
 - Experimental validation of the spray evaporation model (adaption if necessary) the described results in this report show that the simulation tool is working, but results might deviate from a real system.
 - Identification of location with beneficial ambient conditions. Nairobi has a high relative humidity (average over the year: 69%), which limits the applicability of spray evaporation (higher process temperatures are required in comparison to location with lower air humidity)
 - For each application scenario (type of heat source, climatic conditions), a comprehensive sensitivity study would need to be performed to elucidate if a evaporation ratio of 90% is possible to reach.



• For a stand alone solution, an assessment tool for solar electricity production was built and tested in Python. More studies are recommended, including assessment of further renewable energy technologies like solar thermal collectors, wind power and heat pumps.

For sustainable implementation of the technology, the specifications of the solution have to be determined - system design with local people and stakeholders. The value of salt, as a result of zero-liquid discharge desalination, was identified regarding diversity of applications and their respective value drivers.



8. References

- [1] DesalData, 2018. GWI/DESALDATA. Available at:. https://www.desaldata.com/
- [2] Jones E, Qadir M, van Vliet MTH, Smakhtin V, Kang S mu. The state of desalination and brine production: A global outlook. Sci Total Environ 2019;657:1343–56. https://doi.org/10.1016/j.scitotenv.2018.12.076.
- [3] Yuan G. Expert interview with Dr. Goufeng Yuan from the Institute of Electrical Engineering, Chinese Academy of Sciences, Beining, China. April 2020.
- [4] Hoque S, Alexander T, Gurian PL. INNOVATIVE INLAND BRINE DISPOSAL OPTIONS. Annual Conference and Exposition of the American Water Works Association, 2008.
- [5] Xu P, Cath TY, Robertson AP, Reinhard M, Leckie JO, Drewes JE. Critical review of desalination concentrate management, treatment and beneficial use. Environ Eng Sci 2013;30:502–14. https://doi.org/10.1089/ees.2012.0348.
- [6] Mathioulakis E, Belessiotis V, Delyannis E. Desalination by using alternative energy: Review and state-of-the-art. Desalination 2007;203:346–65. https://doi.org/10.1016/j.desal.2006.03.531.
- [7] Houcine I, Benamara M, Guizani A, Maâlej M. Pilot plant testing of a new solar desalination process by a multiple-effect-humidification technique 2006;196:105–24. https://doi.org/10.1016/j.desal.2005.11.022.
- [8] JAKOB BERG JOHANSEN. Desalination of sea water using solar energy. Master thesis. 2014. Technical University of Denmark.
- [9] Yuan G. et al., Expirimental investigation of a humidification-dehumidification system (Chinese research article), ACTA Energiae Solaris Sinica, Vol. 37, No.12, 2016.
- [10] Saltworks Technologies Inc., SaltMaker-MultiEffect Closed Evaporator Crystallizer.

 Product data sheet. Available at: https:saltworkstech.com, [accessed in March 2020].
- [11] Xuening F, Lei C, Yuman D, Min J, Jinping F. CFD modeling and analysis of brine spray evaporation system integrated with solar collector. DES 2015;366:139–45. https://doi.org/10.1016/j.desal.2015.02.027.
- [12] Kalogirou SA. Design of a new spray-type seawater evaporator. Desalination 2001;139:345–52. https://doi.org/10.1016/S0011-9164(01)00329-0.
- [13] Seawater properties reference database, https://www.britannica.com/science/seawater/Dissolved-inorganic-substances, accessed in April 2020.



- [14] JONES, Edward, et al. The state of desalination and brine production: A global outlook. *Science of the Total Environment*, 2019, 657: 1343-1356.
- [15] GEBOERS, E. The Salt Project. 2015.
- [16] http://www.emergingobjects.com/portfolio/
- [17] https://store.h2gopurifier.com/collections/products/products/h2go-purifier-global
- [18] Dindi, A., Quang, D. V., AlNashef, I., & Abu-Zahra, M. R. A process for combined CO2 utilization and treatment of desalination reject brine. Desalination, 442, 62-74. 2018.
- [19] Protheroe, M. D., Al-Jumaily, A., & Nates, R. J. Prediction of droplet evaporation characteristics of nebuliser based humidication and drug delivery devices. In: International Journal of Heat and Mass Transfer, 2013, 60, p:772-780.
- [20] Spraying Systems. Automatic and air atomising spray nozzles. Product catalogue, Product catalogue, Spraying Sysems Co provided by MT Spray A/S, 2020.
- [21] Holmgren WF, Hanses CW, Mikofski MA. pvlib python: a python package for modeling solar energy systems. In: The Journal of Open Source Software, 2018
- [22] Huld T, Mueller R, Gambardella A. A new solar radiation database for estimating PV performance in Europe and Africa. In: Solar Energy; 2012. p. 1803-1815.
- [23] https://www.homedepot.com/p/Grape-Solar-3600-Watt-Expandable-Monocrystalline-Grid-Tied-Solar-Power-Kit-GS-12-PANEL-KIT-SE/311605699
- [24] https://www.homedepot.com/p/Grape-Solar-6-000-Watt-Expandable-Monocrystalline-PV-Grid-Tied-Solar-Power-Kit-GS-20-PANEL-KIT-SE/311605700
- [25] Marion B. Overview of the PV Module Model in PVWatts. In: PV Performance Modeling Workshop. 2010.
- [26] King DL, Gonzalez S, Galbraith GM, Boyson WE. Performance Model for Grid-Connected Photovoltaic Inverters. In: Sandia Report 2007.





BYG R-446 October 2020

ISBN: 87-7877-5477

Department of Civil Engineering, DTU Brovej, Building 118 2800 Kgs. Lyngby

www.byg.dtu.dk/english

Tel: 4525 1700